The Importance of the lipid composition in Peroxisome Biology

Research Project – 1 September 2013 – June 2014

ChandhuruJagadeesan

Student no: S2581965

Supervisor: Adam Kawałek

Professor: Dr. I.J. van der Klei

June 2014

University of Groningen, Department of Molecular Cell Biology, Nijenborgh 7,

9747 AG Groningen, The Netherlands

Acknowledgements

In the first place I would like to thank Prof.Dr. Ida J. van der Klei, for giving me an opportunity to work in this enthusiastic group.

I would like to thank my supervisor Adam Kawałek for his excellent assistance, advice, patience, proper planning to avoid midnight experiments and teaching me everything.

I would like thank Arjen for his valuable help in confocal microscopy.

I would like to thank all the members of the Molecular Cell Biology group for giving their valuable support and suggestions to finish my project.

Finally I would like to thank my parents and friends for their inspiration.

Table of Contents

Introduction

Peroxisomes are single membrane bound multifunctional organelles which are found in most eukaryotes except the Apicomplexa and the amitochondrial parasites [1]. The specific feature of this organelle is the presence H_2O_2 producing oxidases; along with catalase to detoxify this toxic by-product. Peroxisomes also contain many other metabolic enzymes which sometimes form electron-dense crystalloid cores. These micro bodies are 0.1-1µm in diameter. Their function, number and shape vary depending on the organism, cell type and the environmental conditions. The most common and evolutionarily conserved functions of these organelles include the β-oxidation of fatty acids and detoxification of H_2O_2 [2]. The specialized functions are species specific. These include metabolism of unusual carbon and nitrogen sources like D-amino acids, purines, oleic acid in *Saccharomyces cerevisiae*, methanol in methylotrophic yeast, penicillin production in *Pencillium chryosogenum* [3], Woronin body biogenesis in filamentous fungi [4], photorespiration in plants [5], synthesis of plasmalogen and short term anti-viral protection during viral infection in humans [6, 7]. The metabolic processes shared between peroxisomes and other cellular compartments like mitochondria, chloroplast and cytosol are responsible for maintaining cellular homeostasis [8].

Biogenesis of peroxisomes

Like, chloroplast and mitochondria peroxisomes were initially considered as autonomous organelles which are formed from pre-existing ones by fission. Later studies proved that they can also be derived from endoplasmic reticulum (ER) by *de novo* formation when the cells are devoid of them [9]. In yeast there are 31 genes, termed *PEX* which are important for biogenesis and division of peroxisomes. Extensive research in different organisms were conducted in order to understand the mechanism of peroxisome biogenesis, but they often led to many discrepancies and they haven't answered all the questions regarding the molecular details of peroxisomes formation. Currently there are two models – the vesicle fusion model

and growth and division model (reviewed in [10]). According to the vesicle fusion model there are two distinct ER-derived vesicles in *S. cerevisiae*, one type of vesicle has the docking complex proteins (Pex13, Pex14, Pex17) and other vesicle contains the RING-finger complex proteins (Pex2, Pex10 and Pex12). These two heterotypic vesicle fuse to form import competent peroxisomal structure [11]. Growth and division model proposes that peroxisomes form by fission from pre-existing ones and peroxisomal membrane proteins (PMPs) containing vesicles from the ER fuse with them to form functional peroxisomes which can grow further and divide [12].

Matrix protein import

Peroxisomes are devoid of DNA and protein synthesis machinery. Peroxisomal matrix proteins are synthesized on free ribosomes in the cytosol and imported in folded, oligomeric and cofactor-bound form. The peroxisomal matrix proteins usually have either one of the two known Peroxisomal Targeting Signals (PTS1 or PTS2). The import mechanism of PTS1 containing matrix proteins is well understood. The PTS1 signal peptide is about 12 amino acids long present at the C-terminus of the protein [13]. The last three amino acids have a consensus sequence (S/A/C)-(K/R/H)-(L/M). PTS1 is recognized and bound by Pex5. The PTS2 signal peptide is located within the N-terminal part of the protein. It has a consensus sequence (R/K)-(L/V/I)-X_5-(H/Q)-(L/A) [14]. Matrix proteins having PTS2 signal binds to Pex7 with the help of co-receptors Pex18 and Pex21 in *S. cerevisiae* [15] or Pex20 in *H. polymorpha* [16]. The receptor-cargo complex binds to a docking complex present at the peroxisomal membrane. The docking complex in yeast is made of peroxisomal membrane proteins (PMPs) Pex13, Pex14 and Pex17 [17]. The receptor-cargo complex interacts with docking complex to form a transient pore and translocate the cargo to the peroxisomal matrix [18]. Planar lipid layer studies have also shown that Pex5 along with Pex14 integrates into membrane to form ion-conducting channel [19]. After the cargo release, Pex5 is

mono-ubiquitylated by the RING-finger complex proteins (Pex2, Pex10 and Pex12) along with Pex22 and Pex4 [20]. This enables Pex5 to be recycled back to the cytosol where the ubiquitin moiety is removed [21]. When receptor recycling is dysfunctional Pex5 is poly-ubiquitylated by Ubc4 and Pex2 which directs it to the proteasome for degradation [21].This pathway is known as RADAR (Receptor Accumulation and Degradation in the Absence of Recycling) pathway. Mono-ubiquitylated or poly-ubiquitylated Pex5 is removed from the membrane by AAA (ATPase Associated with various cellular Activities family) peroxins Pex1 and Pex6 in a ATP dependent manner[22]. Pex1 and Pex6 are associated with membrane via Pex15 in *S. cerevisiae* and Pex26 in *H. polymorpha*. In mammalian cells the PTS2 mediated translocation depends on Pex5 (known as Pex5L) which associates with Pex7. This shows that at least in mammalian cells PTS2 containing matrix proteins are imported through same mechanism as PTS1 containing matrix proteins.

Membrane protein insertion

Import mechanism of membrane proteins is not well understood. PMPs are divided into two classes: class I PMPs which can be directly targeted to peroxisomes and class II PMPs which could also be targeted to the peroxisomes with the assistance of endoplasmic reticulum (ER). Class I PMPs are synthesized on the free ribosomes in the cytosol and are recognized by the soluble receptor, Pex19. The C-terminal of the Pex19 has an α-helical domain which binds with the membrane PTS (mPTS) [23, 24]. Pex19-cargo PMP complex binds to the membrane bound Pex3 and the cargo PMP is inserted into the membrane. In yeast, class II PMPs are thought to be inserted into the ER by the Sec61 translocon[25, 26] and the GET complex [26, 27], which then buds from the ER to form vesicles. These vesicles are thought to fuse with pre-mature peroxisomes to form functional peroxisomes.

Peroxisome proliferation

Peroxisomes are usually spherical in shape, but they can change to even form reticula structure in certain cell types [28, 29]. In yeast, the number and size of the peroxisomes vary according to the environmental conditions. Growth of the cells in peroxisome inducing conditions like medium containing oleic acid (*S. cerevisiae*) and methanol (*H. polymorpha*), results in up regulation of *PEX* genes and proliferation of these organelles. *H. polymorpha* cells usually contain 1 small peroxisome when cells are grown in glucose containing medium. Growth in methanol medium results in higher number of bigger crystalline core containing organelle. Similar induction is observed when *S. cerevisiae* is grown in oleic acid. Deletion of *PEX* genes doesn't result in a lethal phenotype in yeast. These attributes makes them a good model organism to study the biogenesis of peroxisomes.

The regulation of peroxisome number is highly complex and coordinated with other process like fission, *de novo* formation, segregation and degradation. The molecular mechanism of peroxisome fission in yeast and mammalian cells is thought to be conserved. First step of this process involves tubulation/elongation of the organelle by Pex11 family members. Based on the *in vitro* studies Opalinski et al showed that the N-terminal amphipathic helix is responsible for tubulation [30]. This step is followed by anchoring of the Dynamin related proteins (DRP) interacting proteins like Fis1 to the membrane [31, 32]. The final step of membrane scission is mediated by GTPases from DRP family like Vps1 and Dnm1 in *S. cerevisiae* [33, 34] and Dnm1 in *H. polymorpha*. Fission results in formation of small daughter peroxisome. The daughter peroxisome incorporates lipids and PMPs to grow into a mature functional peroxisome with a specific set of peroxisomal matrix proteins.

Table 1. Phospholipid composition of peroxisomal membrane in different organisms

Organism	Medium	Mol% of Total Phospholipids							Ref.
		PC	PE	PI	PS	CL	PA	Others	
S.cerevisiae FY1679	Glucose	39·8	17·4	22·0	2·5	2·7	6·1	Nd	[35]
S.cerevisiae (D273-10B)	oleate	48.2	22.9	15.8	4.5	7.0	1.6	Nd	[36]
Castor bean	-	54	29	10	2	2	-	-	[37]
Rat liver cells	-	56.4	27.5	4.7	3.0	-	-	Nd	[38]
Trypanosomac ruzi Glycosomes	-	13.75	61.1	0.15	22.91	-	-	Nd	[39]
P.pastoris	Methanol	54.4	27.6	6.3	3.7	3.9	1.8	0.7	[40]
P.pastoris	Oleate	52.4	26.6	6.1	6.7	2.3	3.2	0.1	[40]
S.cerevisiae FY1679	YPO	49	17	21	5	1	-	7	[41]

PC, Phosphatidylcholine; PE, Phosphatidylethanolamine;PI, Phosphatidylinositol; PS, Phosphatidylserine; CL, Cardiolipin; PA, Phosphatidic acid; others, other phospholipids such as lyso-phosphalipids, phosphatidylglycerol, Phosphatidylmethylethanolamine

Lipid composition of peroxisomes

The most abundant phospholipids in the peroxisomal membrane include phosphatidylcholine (PC), phosphatidylethanolamine (PE) and phosphatidylinositol (PI) **(Table. 1)**. In yeast, the phospholipid composition of the peroxisomal membrane as well as the fatty-acid composition of their corresponding acyl chains strongly depends on carbon source used for growth [40]. Remarkably yeast peroxisomes were found to contain substantial amount of cardiolipin (CL) [40]. CL was not found or was under the detection limit in peroxisomes isolated form *Candida tropicalis*[42]. Analysis of rat liver peroxisomes also did not reveal the presence of CL [38, 43]. A careful examination of *A. thaliana* cells stained with a CL specific dye

nonylacridine orange (NAO) did not reveal peroxisomal staining [44], but CL was detected in peroxisomes isolated from castor bean [37]. Cardiolipin is synthetized and predominantly localized in mitochondrial membranes (for review see [45, 46]). The presence of cardiolipin in yeast peroxisomes is controversial as obtaining pure fractions of peroxisomes by density gradient centrifugation without mitochondrial contamination is difficult. Hence, different experimental approach is needed to confirm the presence of CL in the peroxisomal membranes.

Cardiolipin and its molecular functions

Cardiolipin is a special negatively charged lipid composed of two 1,2 diacylphosphatidate moieties that are connected to 1 and 3–hydroxyl groups of a single glycerol head group (**Fig. 1A**). The cross-sectional area of the hydrophilic head group is smaller than the hydrophobic tail group which makes this lipid cone shaped. In water CL forms aggregates with a negative curvature called inverted hexagonal phase (H_{II}) (**Fig. 1D**). This membrane structure can be formed only when the repulsive force between the two phosphate group is balanced by the presence of divalent metal ions or proteins (at low pH) [47]. This makes the CL to switch between lamellar and non-lamellar structure, which is thought to help in mitochondrial fission and fusion [48, 49]. CL helps in maintaining the stability and activity of the respiratory complexes [50]. It helps in import and assembly of inner membrane proteins [51]. Additionally, CL plays a major role in apoptosis [52]. Deficiency of CL also results in change in membrane potential of the inner mitochondrial membrane [53–55]. The deleterious effects of CL deficiency outside the mitochondria include perturbation of the PKC-Slt2 cell integrity and high osmolarity glycerol (HOG) signaling pathways and decreased vacuolar function [56–59]. CL deficiency has been found to decrease the longevity in yeast cells [59]. The importance of CL in man is highlighted by the fact that the loss of CL synthesizing gene results in Barth syndrome.

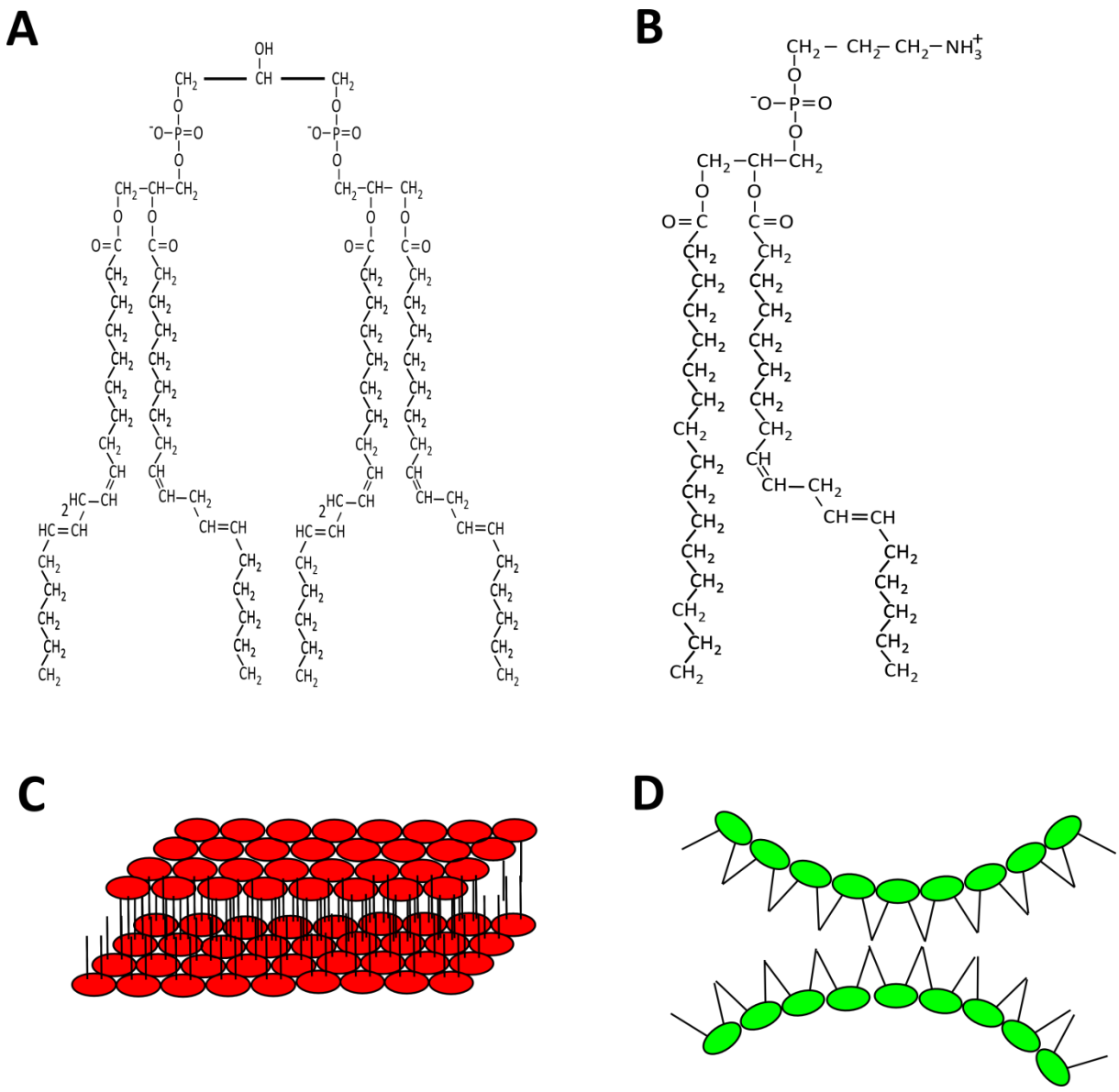

Figure 1. Structure of cardiolipin (CL) **(A)**. Structure of phosphatidylethanolamine (PE) **(B)**. the structure of CL and PE varies with the length of fatty acid chain. The above mentioned structure is just an representative structure of CL and PE. Bilayer formation by cylindrical lipids **(C).** Inverted hexagonal structure formed by CL and PE **(D)**.

PE and its molecular functions

PE is also a non-bilayer forming lipids, which forms inverted hexagonal (H_{II}) membrane structure in the hydrated environment (**Fig. 1AD**). Akin to CL, propensity of PE to form this structure depends on the number of double bonds and length of the acyl chains. The longer the acyl chain and the more the number of double bonds, the easier to form inverted hexagonal structure [60, 61]. PE has the ability to stabilize respiratory protein complexes and acts as

chaperone during protein import [62, 63]. Additionally, PE plays an important role in autophagy. Atg8 is lipidated by the addition of PE in a reversible manner to control the membrane dynamics during autophagy [64]. Depletion of PE results in loss of mitochondrial DNA and altered morphology in yeast and mammalian cells [62, 63].

Remarkably, lack of CL is balanced by increasing the production of PE and PG inside the cell. PG is negatively charged like CL and PE has the ability to form non-lamellar structure [61, 65]. Similarly lack PE is compensated by CL and phosphatidic acid (PA). Deletion of both *CRD1* and *PSD1* results in lethal phenotype which indicates that CL and PE have overlapping functions[49].

Biosynthesis of CL and PE

The biosynthesis of glycerophospolipids in yeast is similar to higher eukaryotes. PA serves as the central metabolite in *de novo* synthesis of all the phospholipids **(Fig. 2)**. Glycerol-3-phosphate(G3P) and dihydroxyacetone phosphate (DHAP) is converted to lyso-PA, catalyzed by acyl-transferases (Gat1, Gat2, Sct1, Gpt2) and reductase (Ayr1p) [66, 67]. Lyso-PA is converted to PA by the transfer of acyl group from acyl-CoA by the action of Slc1p, Slc4p, Loa1p and Ale1 [68].

PA is converted into cytidine phosphate diacyl glycerol (CDP-DAG) by Cds1p present in both mitochondria and ER, with cytidine triphosphate (CTP) as CDP donor [69, 70]. Phosphatidylglycerolphosphate synthase (Pgs1p), localized to mitochondria uses CDP-DAG and G3P as substrates to synthesize phosphatidylglycerolphosphate (PGP) [71]. Furthermore phosphate group is removed from PGP by PGP phosphatase Gep4 to synthesize phosphatidylglycerate (PG) [72]. PG is further converted to cardiolipin by CL synthase (Crd1) [73]. The acyl chain in the CL can be trimmed according to the requirement by the enzyme Taz1.

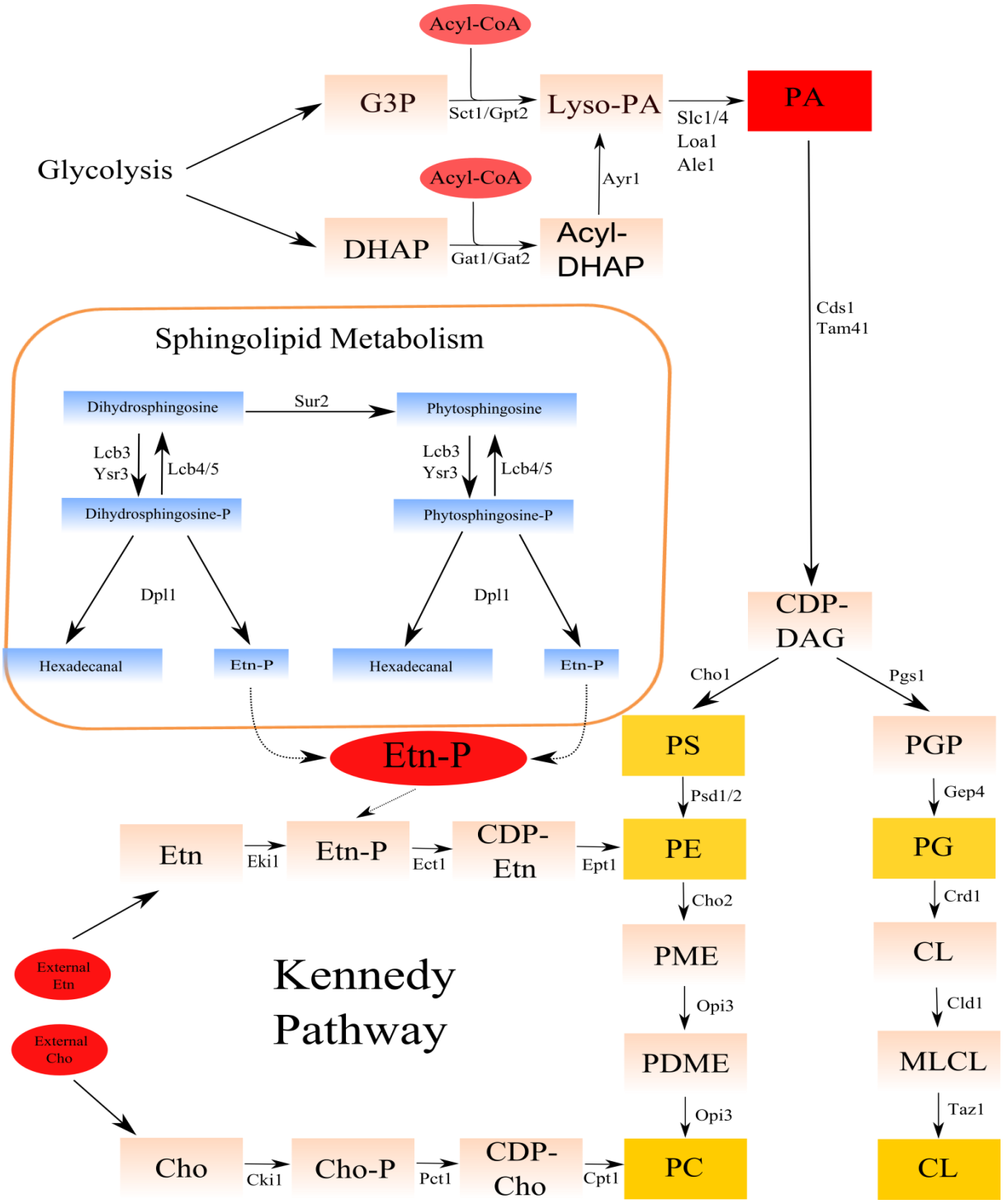

Figure 2. Biosynthesis of cardiolipin and phosphatidylethanolamine in Yeast. The different branches of biosynthesis, the lipid products and the enzymes involved are described in the text. G3P, glycerol-3-phosphate; DHAP, dihydroxyacetone phosphate; acyl-DHAP, acyl dihydroxyacetone phosphate; Lyso-PA, lysophosphatidic acid; PA, phosphatidic acid; CDP-DAG, cytidinediphosphatediacylglycerol; PS, phosphatidylserine; PGP, phosphatidylglycerolphosphate; PE, phosphatidylethanolamine; PG, phosphatidylglycerol; PME, phosphatidylmethylethanolamine; CL, cardiolipin; PDME, phosphatidyldimethylethanolamine; MLCL, monolysocardiolipin; PC, phosphatidylcholine; Cho, Choline; Cho-P, phosphocholine; CDP-Cho, cytidinediphosphatecholine; Etn, ethanolamine; Etn-P, phosphoethanolamine; CDP-Etn, cytidinediphosphateethanolamine.

PE is synthesized by three different pathways. Phosphatidylserine (PS) synthesized from CDP-DAG by Cho1p is used as substrate for PE synthesis [74]. PE is synthesized by decarboxylation of PS, catalyzed by phosphatidylserine decarboxylase 1 (Psd1) present in the inner mitochondrial membrane and phosphatidylserinedecarboxylase 2 (Psd2) in the Golgi complex [75, 76]. Psd1 is the major route of PE synthesis in *S. cerevisiae* as it represents 80% of the total cellular Psd activity. *psd1* cells display severe growth defect when grown on non-fermentable carbon sources [62]. The third pathway that contributes to PE synthesis is the CDP-ethanolamine/choline pathway also known as Kennedy pathway. Ethanolamine taken up from the medium is converted to phosphoethanolamine (Etn-P) by Eki1 [77]. Etn-P is converted to CDP-ethanolamine by Ect1 [78]. Phosphoethanolamine moiety is transferred from CDP-ethanolamine to DAG by Ept1 to from PE [79]. The CDP-ethanolamine branch of Kennedy pathway is redundant with the CDP-choline branch. Eki1 and Ect1 share overlapping substrate specificity with the Cki1 and Cpt1 of CDP-Choline branch [77, 80].

Sphingolipid metabolism contributes to a minor fraction of PE biosynthesis. Phytosphingosine-P and dihydroxysphingosine-P, products of sphingolipid degradation are converted to Etn-P and hexadecanal by dihydroxysphingosine-1-phosphate lyase Dpl1p [81, 82]. This Etn-P enters the Kennedy pathway to produce PE. The contribution of Dpl1p to PE synthesis is very low since the double deletion *psd1 psd2* cells are not viable without the exogenous choline or ethanolamine [62]. Thus, the catalytic function of all these enzymes localized to different cellular compartments are necessary to maintain the lipid composition in all the membranes.

Transport of lipids to peroxisomes

Peroxisomes lack the ability to synthesize lipids and therefore rely on lipid transport from other cellular compartments. The mechanism of phospholipids transport from the site of synthesis (ER, mitochondria and Golgi complex) to the peroxisomes is still unknown. Both

vesicular and non-vesicular (protein dependent and independent) mechanism of lipid transport has been thought to be suggested in lipid transport to these organelles. Lipids could be transported to the peroxisomes along with the PMPs in vesicles. In *S. cerevisiae* Sec16 and Sec18 dependent vesicular transport pathway was not required to transport lipids from the ER to peroxisomes [83]. In yeast cytosolic Lipid Transfer Proteins (LTPs) can transport PI, PC, PS and PE between compartments [84]. In mammalian cells vesicular transport pathway was also described between mitochondria and peroxisomes [83]. Apart from vesicular transport routes, also contact sites between the organelles has been implicated in lipid transport [86]. Proximity of 2 membrane bilayers facilitates flipping of lipids from one membrane to another. Mitochondria-ER contact sites have been known for more than 50 years through the ultra-structural electron microscopy and its role in lipid transport and the proteins required for functioning of the contact sites has been elucidated (reviewed by[87–89]). In *S. cerevisiae* existence of ER-Mitochondria contact sites also known as MAMs (Mitochondria Associated Membrane) were clearly shown with the help of fluorescent microscopy and computer aided 3D reconstruction of electron tomographs[90]. Based on computer aided 3D reconstruction of electron tomographs Rosenberger et al have shown that peroxisomes were in close contact with other cell organelles like ER and mitochondria. The distance between the membranes in the contact sites as 4-45 nm [41]. Existence of contact sites between ER, Mitochondria and peroxisomes is highly relevant for the exchange of fatty acids during the β-oxidation and transport of phospholipids. Further studies on the contact sites will shed light on their roles in lipid transport and other functions.

In this study we investigated the highly speculative role of CL in the peroxisomal membrane by analyzing peroxisome abundance in CL deficient yeast strains. Furthermore, we analyzed the effect of PE depletion on the peroxisome abundances in the yeast.

Materials and methods

Strains and growth conditions

The *S. cerevisiae* strains used in this study are listed in Table 2. Cells were grown at 30˚C either in mineral medium (w/o yeast extract) containing 0.5% glucose or 0.1% glucose, 0.1% oleate and 0.05% tween 80. Whenever required medium was supplemented with leucine (30 µg/ml), histidine (20 µg/ml), uracil (30 µg/ml) or lysine (30 µg/ml). Selection of yeast transformants was performed on YPD agar plates supplemented with 300 µg/ml hygromycin B, 100 µg/ml gentamycin, 100 µg/ml nourseothricin or 200 µg/ml zeocine.

The *H. polymorpha* strains used in this study are listed in Table 3. Cells were grown in mineral medium [91] supplemented with either 0.5% glucose or 0.5% methanol as carbon sources and 0.25% ammonium sulphate as a nitrogen source. For chemostat experiments, cells were pre-cultivated in mineral medium containing 0.25% glucose and 0.25% ammonium sulphate. Culture conditions for chemostat: temperature 37˚C, pH 5 and dilution rate of 0.1. The feed medium contained mineral medium with 0.5% methanol and 0.25% ammonium sulphate. When required leucine was added to a final concentration of 60 µg/ml. Selection of yeast transformants was performed on YPD agar plates supplemented with 300 µg/ml hygromycin B, 200 µg/ml zeocine. For cloning purposes, *E. coli* DH5α was used. Transformed bacteria were screened on LB agar plates supplemented with 100 µg/ml ampicillin or 50 µg/ml kanamycin. For plasmid isolation, bacteria were grown in LB media at 37˚C supplemented with appropriate antibiotics.

Cloning and construction of yeast strains

The plasmids and primers used in this study is listed in **Table S3**, **Table S4** and **Table S5**. All the cloning for *H. polymorpha* was performed using Gateway technology (Invitrogen). Transformation of *H. polymorpha* by electroporation as described previously [92].

Transformation of *S. cerevisiae* was performed by Li-Ac method [93]. All deletions and integrations in *H. polymorpha* were confirmed by PCR and southern blotting.

Table 2. *S. cerevisiae* strains used in this study

Strain	Description	Reference
Wild-type (WT)	BY4742 MATα *his3Δ1 leu2Δ0 lys2Δ0 ura3Δ0*	EUROSCARF
crd1	BY4742 *CRD1*::kanMX4	EUROSCARF
crd1 GFP-SKL	*crd1* P_{MET25} GFP-SKL	This study
psd1	BY4742 *PSD1*::kanMX4	This study
psd1 GFP-SKL	*psd1* P_{MET25} GFP-SKL	This study
psd2	BY4742 *PSD2*::kanMX4	EUROSCARF
psd2 GFP-SKL	*psd2* P_{MET25} GFP-SKL	This study
cki1 eki1 dpl1	BY4742 *EKI1*::kanMX4 *CKI1*::HPH*DPL1*::NAT	This study
cki1 eki1 dpl1 GFP-SKL	*cki1 eki1 dpl1* P_{MET25} GFP-SKL	This study

Construction of *S. cerevisiae* deletion strains

PCR based deletion strategy was used and primers were designed to have a tail of 50 nucleotides homologous to the desired gene of interest. The yeast deletion mutant *psd1* was constructed by replacement of chromosomal *PSD1* gene. Primers ScPSD1_del_F and ScPSD1_del_R were used to amplify the gentamicin cassette using pUG6 as the template. This was amplified using primers ScPSD2_del_F and ScPSD2_del_R and pENTR221_NAT as a template. *cki1 eki1 dpl1* mutant was constructed by replacing the chromosomal *EKI1*, *CKI1* and *DPL1* gene with gentamicin resistance cassette, hygromycin resistance cassette and nourseothricin resistance cassette, respectively. Gentamicin resistance cassette was amplified by using primers ScEKI1_del_F and ScEKI1_del_R and pUG6 as the template. Hygromycinresistance cassette was amplified by using primers ScCKI1_del_F and ScCKI1_del_R and pENTR_221_HPH as the template. Nourseothricinresistance cassette was

amplified by using primers ScDPL1_del_F and ScDPL1_del_F and pENTR_221_HPH as the template. These cassettes were transformed into respective strains and colonies were selected on YPD plates and colony PCR was done to confirm the deletion.

Table 3. *H. polymorpha* strains used in this study

Strain	Description	Reference
Wild-type (WT)	NCYC 495 *KU80*::*URA3*	[94]
WT. *PMP47*-mGFP	WT P_{PMP47}*PMP47*-mGFP	This study
WT. *PMP47*-mGFP/GFP-SKL	WT P_{PMP47}*PMP47*-mGFP/P_{TEF1} GFP-SKL	This study
crd1	NCYC 495 *KU80*::*URA3 CRD1::HPH*	This study
crd1 PMP47-mGFP	*crd1* P_{PMP47}*PMP47*-mGFP	This study
crd1 PMP47-mGFP/GFP-SKL	*crd1* P_{PMP47}*PMP47*-mGFP/P_{TEF1} GFP-SKL	This study
psd1	NCYC 495 *KU80*::*URA3 PSD1::HPH*	This study
psd1 PMP47-mGFP	*psd1* P_{PMP47}*PMP47*-mGFP	This study
psd1 PMP47-mGFP/GFP-SKL	*psd1* P_{PMP47}*PMP47*-mGFP/P_{TEF1} GFP-SKL	This study
psd2	NCYC 495 *KU80*::*URA3 PSD2::HPH*	This study
psd2 PMP47-mGFP	*psd2* P_{PMP47}*PMP47*-mGFP	This study
psd2 PMP47-mGFP/GFP-SKL	*psd2* P_{PMP47}*PMP47*-mGFP/P_{TEF1} GFP-SKL	This study

Construction of *H. polymorphacrd1* deletion strain

Crd1 protein sequence was obtained from *Saccharomyces* genome database (SGD) and blasted in *Hansenulapolymorpha* genome database to find the corresponding gene homologues. Due to dense ORF distribution in *CRD1* homologue (protein ID: 16899) map only 50bp was deleted and replaced by hygromycin B resistance cassette (HPH), start codon was changed to stop codon. To this end the first region -1234 to 0 of the *CRD1* gene was amplified by performing two PCRs, using primers CRD1_del5F and CRD1_OL_R and CRD1_OL_F and CRD1_del5R. These two products were gel extracted and overlap PCR was

performed using primers CRD1_del5F and CRD1_del5R containing attB sites. This was recombined with pDONR41 yielding pENTR_41_5'*CRD1*. At the same time the region +50 to +840 was amplified using primers CRD_del3F and CRD_del3R and recombined with pDONR41 yielding pENTR_23_3'*CRD1*. A deletion cassette containing 5' and 3' fragments of *CRD1* gene and HPH marker was assembled in pDEST43 with a Gateway LR reaction using plasmids pENTR_41_5'*CRD1*, pENTR_221_HPH and pENTR_23_3'*CRD1*. The resulting plasmid pDEST_NAT_CRD1_DEL_HPH was used as a template to amplify the deletion cassette of 3727 bp in a PCR reaction using primers CRD1_del_F and CRD1_del_R. The purified PCR product was transformed into *H. polymorpha ku80* strain and colonies were selected on YPD plates with hygromycin B.

Construction of *H. polymorphapsd1* deletion strain

Psd1 protein sequence was obtained from *Saccharomyces* genome database (SGD) and blasted in *Hansenulapolymorpha* genome database to find the corresponding homologues. *PSD1* homologue (protein ID:15833) comprising nucleotides -296 to +355was replaced by hygromycin B resistance cassette (HPH). To this end the first region -296 to 0 of the *PSD1* gene was amplified using primers PSD1_del5F and PSD1_del5R with attB sites and recombined into pDONR41 yielding pENTR_41_5'*PSD1*. At the same time the region +356 to +1192 was amplified using primers PSD1_del3F and PSD1_del3R and recombined with pDONR41 yielding pENTR_23_3'*PSD1*. A deletion cassette containing 5' and 3' fragments of *PSD1* gene and HPH marker was assembled in pDEST43 with a Gateway LR reaction using plasmids pENTR_41_5'*PSD1*, pENTR_221_HPH and pENTR_23_3'*PSD1*. The resulting plasmid pDEST_NAT_PSD1_DEL_HPH was used as a template to amplify the deletion cassette of 3370 bp in a PCR reaction using primers PSD1_del_F and PSD1_del_R. The purified PCR product was transformed into*H. polymorpha ku80* strain and colonies were selected on YPD plates with hygromycin B.

Construction of *H. polymorphapsd2* deletion strain

Psd2 protein sequence was obtained from *Saccharomyces* genome database (SGD) and blasted in *Hansenulapolymorpha* genome database to find the corresponding homologue. *PSD2*homologue (protein ID:17465) comprising nucleotides -298 to +635was replaced by hygromycin B resistance cassette (HPH). To this end the first region -298 to 0 of the *PSD2* gene was amplified using primers PSD2_del5F and PSD2_del5R with attB sites and recombined into pDONR41 yielding pENTR_41_5'*PSD2*. At the same time the region +636 to +1455 was amplified using primers PSD2_del3F and PSD2_del3R and recombined with pDONR41 yielding pENTR_23_3'*PSD2*. A deletion cassette containing 5' and 3' fragments of *PSD2* gene and HPH marker was assembled in pDEST43 with a Gateway LR reaction using plasmids pENTR_41_5'*PSD2*, pENTR_221_HPH and pENTR_23_3'*PSD2*. The resulting plasmid pDEST_NAT_PSD2_DEL_HPH was used as a template to amplify the deletion cassette of 3568 bp in a PCR reaction using primers PSD2_del_F and PSD2_del_R. The purified PCR product was transformed into *H. polymorpha ku80* strain and colonies were selected on YPD plates with hygromycin B.

Growth curve

The *S. cerevisiae* strains were pre-cultivated using mineral medium (w/o yeast extract) containing 0.5% glucose and 0.25% ammonium sulphate as sole carbon and nitrogen sources. Exponential growing cultures were subsequently shifted to media containing 0.5% glucose or 0.1% glucose, 0.1% oleate and 0.05% tween 80. OD was measured periodically to quantify the doubling time and growth rate.

The *H. polymorpha* strains were pre-cultivated using mineral medium containing 0.25% glucose and 0.25% ammonium sulphate as sole carbon and nitrogen sources. Exponential growing cultures were subsequently shifted to media containing 0.5% glucose or 0.5% methanol. OD was measured periodically to quantify the doubling time and growth rate.

Fluorescence microscopy

Fluorescent microscopy (FM) images were captured using Zeiss confocal microscope 510. GFP fluorescence was analysed by excitation of the cell with a 488 nm argon ion laser, emission was detected using a 500-550 nm bandpass emission filter. For peroxisome quantification in *S. cerevisiae* strains were fixed using 4% formaldehyde in 0.1 M sodium phosphate buffer pH 7.2. In *H. polymorpha* live cells were used to capture image for quantification.

Peroxisome quantification

Image analysis was carried out using Image J. Peroxisome quantification for *H. polymorpha* was done using plugin. In case of *S. cerevisiae* it was done manually.

Results

Cardiolipin deficiency does not reduce the peroxisome number in yeast

To check the impact of cardiolipin deficiency on peroxisomes we analyzed the abundance of these organelles in *S. cerevisiae* and *H. polymorpha* strains deficient in cardiolipin synthase (Crd1).

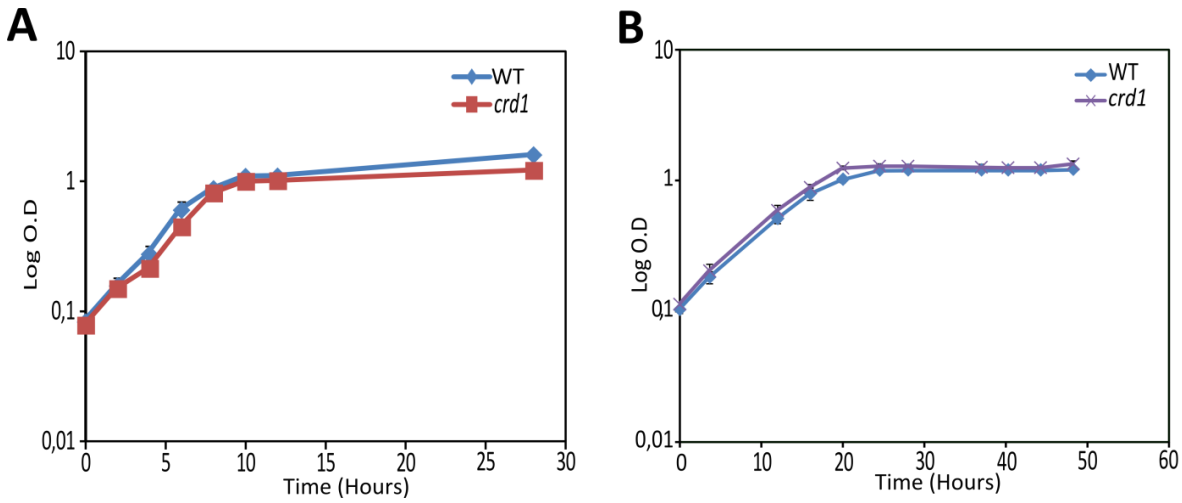

Figure 3. Growth properties of *S. cerevisiae* WT and *crd1* cells. WT and *crd1* cells were grown in medium containing 0.5% glucose **(A)** and 0.1% glucose/0.1% oleate **(B).** The optical density was measured at 600 nm. Data represent mean ± standard deviation from 3 independent cultures.

CRD1 deletion in *S. cerevisiae* did not result in drastic growth defect in the medium containing 0.5% glucose (non-inducing condition) and 0.1% glucose and 0.1% oleate (peroxisome inducing condition) (**Fig. 3AB**). Maximum optical density reached by the *crd1* cells was reduced in the glucose containing medium, accompanied by slightly longer doubling time when compared to wild type cells (**Table. S1**). Doubling time on oleic acid was similar to wild type cells (**Table. S1**). To investigate the effect of CL deficiency on peroxisome number, *S. cerevisiae* WT and *crd1* cells containing peroxisomal marker GFP-SKL under P_{MET25} promoter were grown for 16 hours in the medium containing 0.5% glucose and for 24 hours in peroxisome inducing medium (0.1% glucose/0.1% oleate). Fluorescence microscopy analysis revealed that the GFP spots in *crd1* cells were slightly bigger and more intense when compared with the wild type (**Fig. 4AB**). Peroxisome quantification (counting GFP spots) revealed no differences in the average number of peroxisomes per cell in the *crd1* strain in comparison with wild type(**Table. 4**). Also similar distribution of peroxisome abundance in *crd1* and WT cells was observed (**Figure. 4C**).

Similar analysis with WT and *crd1* cells grown on 0.1% glucose / 0.1% oleate for 24 hours revealed that the average number of peroxisomes in *crd1* cells was slightly higher than in the wild type cells (**Table. 4**). The distribution of peroxisomes in *crd1* strain was characterized by increased number of cells with 6 and 7 peroxisomes when compared to wild type (**Fig. 5C**). Our data indicate that CL deficiency triggered by *CRD1* deletion in S. *cerevisiae* does not reduce the peroxisome number.

Previously, CL was also detected in the peroxisomal fraction of methylotrophs [40]. To analyze the effect of CL deficiency in the methylotrophic yeast *H. polymorpha* we analyzed the strain lacking *CRD1* homologue. *H.polymorpha crd1* cells did not show drastic growth defect in the medium containing 0.5% glucose (**Fig. 6A**). The maximum OD reached by this strain on glucose was slightly lower when compared to the wild type cells (**Table. S2**).

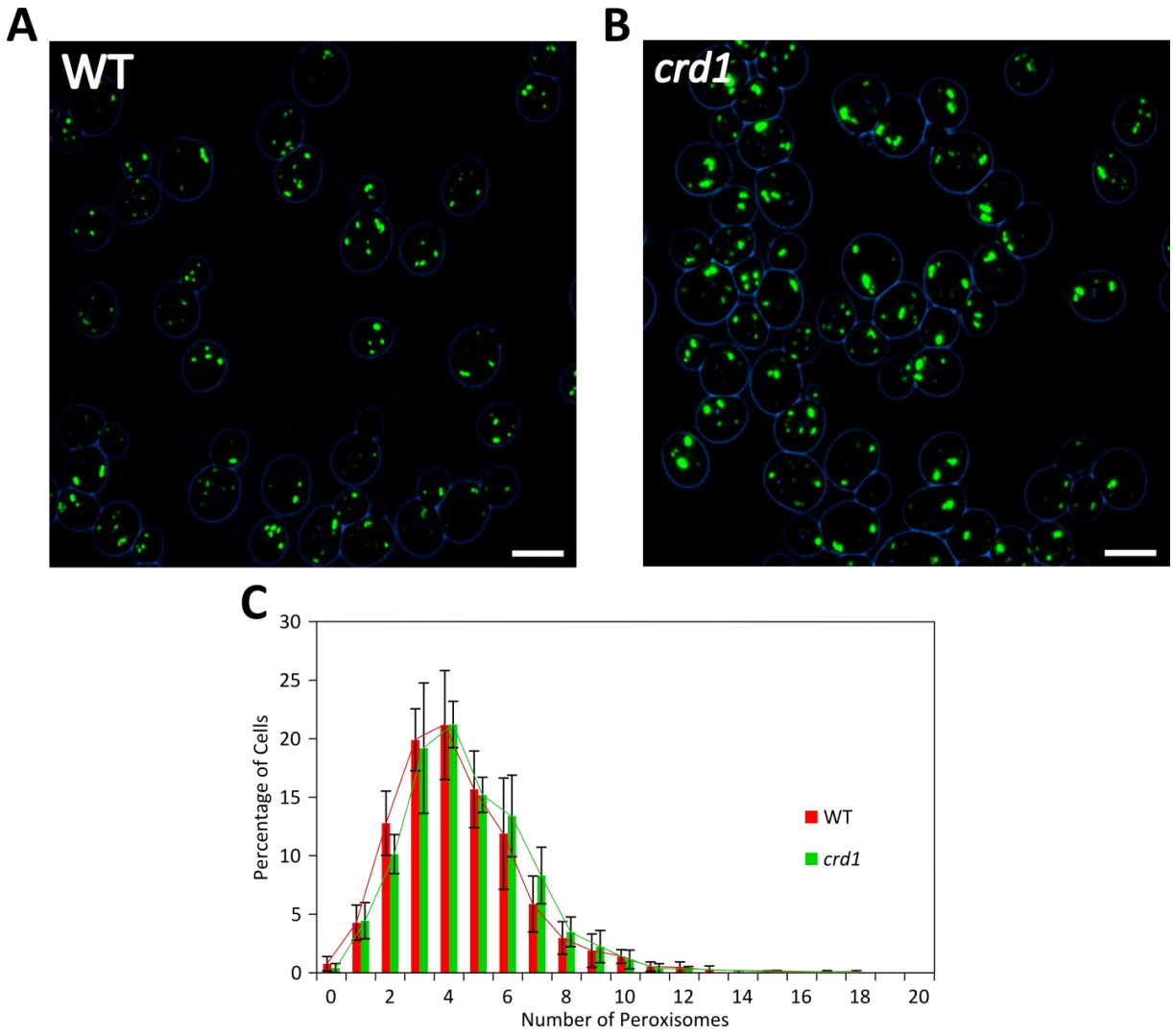

Figure 4. FM analysis of *S. cerevisiae* WT and *crd1* cells. WT and *crd1* expressing GFP-SKL cells were grown for 16 hours in medium containing 0.5% glucose.Fluorescence images of WT **(A)** and *crd1* cells **(B).** Peroxisome distribution in WT and *crd1* cells **(C)**. The above images shown are representative image of WT and *crd1* cells. Data represent average number of peroxisomes ± standard deviation from 7 independent WT and 5 independent *crd1* cultures. The scale bar represents 5 µm.

Remarkably, the doubling time of *crd1* cells was similar to wild type in both 0.5% glucose and 0.5% methanol containing media (**Table. S2**). The growth of *crd1* cells on 0.5% methanol was characterized by longer lag phase and lower maximum OD compared to wild type cells (**Fig. 6B**). To avoid the influence of growth differences on peroxisome quantification WT and *crd1* cells with Pmp47-mGFP were grown in a methanol limited chemostat at equal dilution rate (D=0.1).

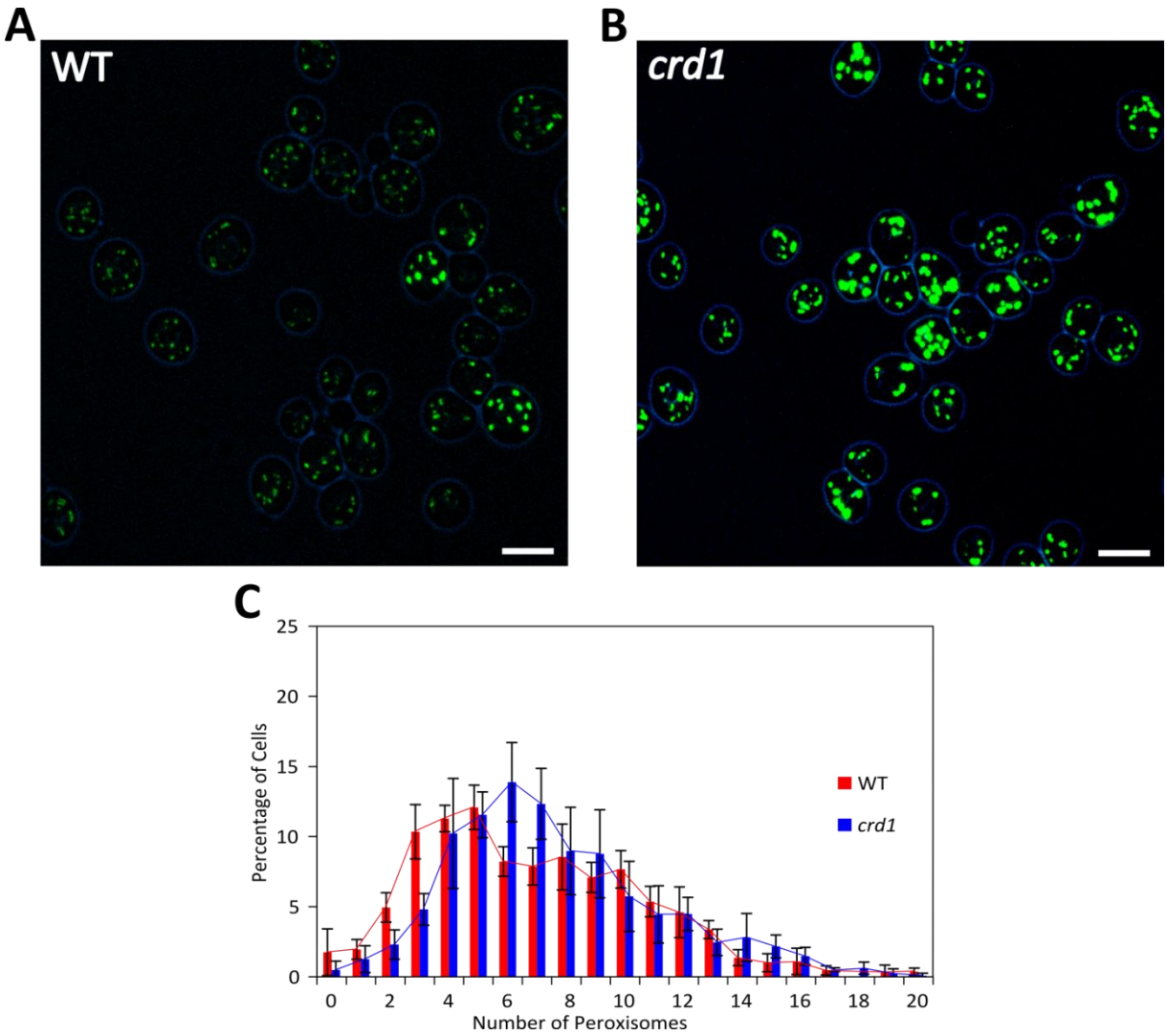

Figure 5. FM analysis of *S. cerevisiae* WT and *crd1* cells. WT and *crd1* cells expressing GFP-SKL were grown for 24 hours in medium containing 0.1% glucose/0.1% oleate.Fluorescence images of WT **(A)** and *crd1* cells **(B).** Peroxisome distribution in WT and *crd1* cells **(C)**. The above images shown are representative image of WT and *crd1* cells. Data represent average number of peroxisomes ± standard deviation from 4 independent WT and *crd1* cultures.The scale bar represents 5 µm.

FM analysis and peroxisome quantification revealed that the average number of peroxisomes per cell and the distribution of peroxisome number in *crd1* strain was same as for wild type (data not shown). Remarkably around 15% of the WT and *crd1* cells did not display Pmp47-mGFP fluorescence (**Fig. 7AB**). To enhance the fluorescent signal and facilitate peroxisome quantification these cells were further transformed with P_{TEF1}-eGFP-SKL. Subsequent growth in methanol limited chemostats and FM analysis of strains expressing 2 peroxisomal markers also did not reveal drastic differences in the average number of peroxisome per cell between

WT and *crd1* cells (**Table. 5**). Similarly, the distribution of peroxisomes in *crd1* cells was similar to wild type (**Fig. 7C**) and 10-15% of the cells did not display GFP fluorescence and thus were considered as peroxisome deficient.

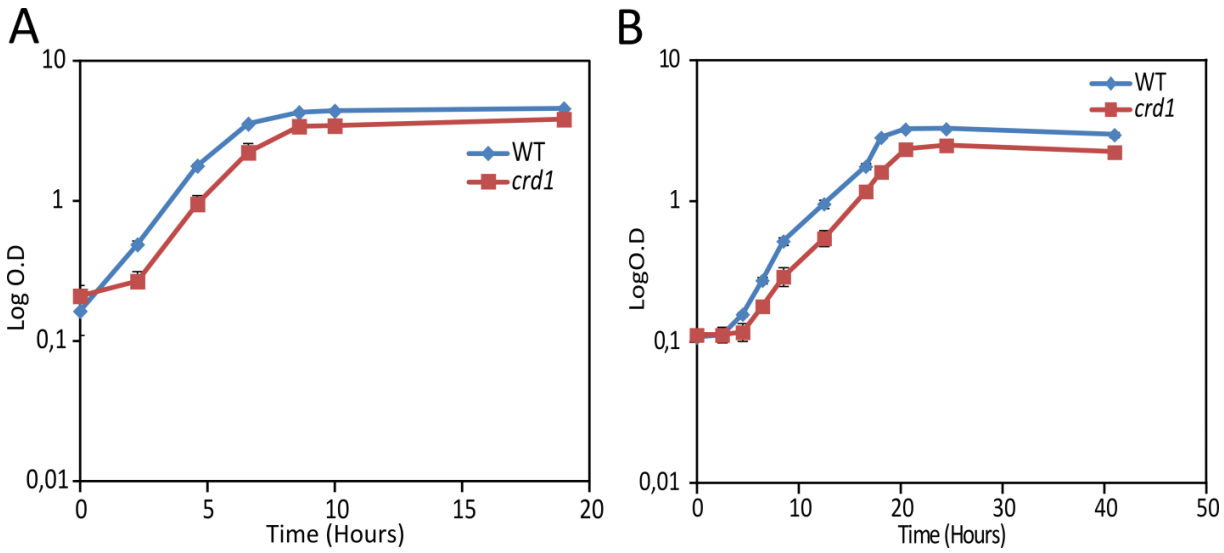

Figure 6. Growth properties of *H. polymorpha* WT and *crd1* cells. WT and *crd1* cells were grown in medium containing 0.5% glucose **(A)** and 0.5% methanol **(B).** The optical density was measured at 600 nm. Data represent mean ± standard deviation from 2 independent cultures.

In order to check whether the cells with no GFP signal are viable or represent dead cells, chemostat grown WT cells containing Pmp47-mGFP/P_{TEF1}-eGFP-SKL were stained with propidium iodide (PI) and analyzed by FACS. Analysis of non-stained (control) cells revealed the presence of two populations of cells with a low and a high GFP intensity (**Fig. 8A**). Upon staining, the population with low GFP signal became PI positive (**Fig. 8B**). These data indicate that the cells without no GFP fluorescence in our analysis are mostly likely representing dead cells. The amount of such cells was similar in WT and *crd1* chemostats, thus their presence is not affecting the outcome of peroxisome quantification. Hence, similar to *S. cerevisiae*, *CRD1* deletion in *H. polymorpha* does not reduce peroxisome abundance.

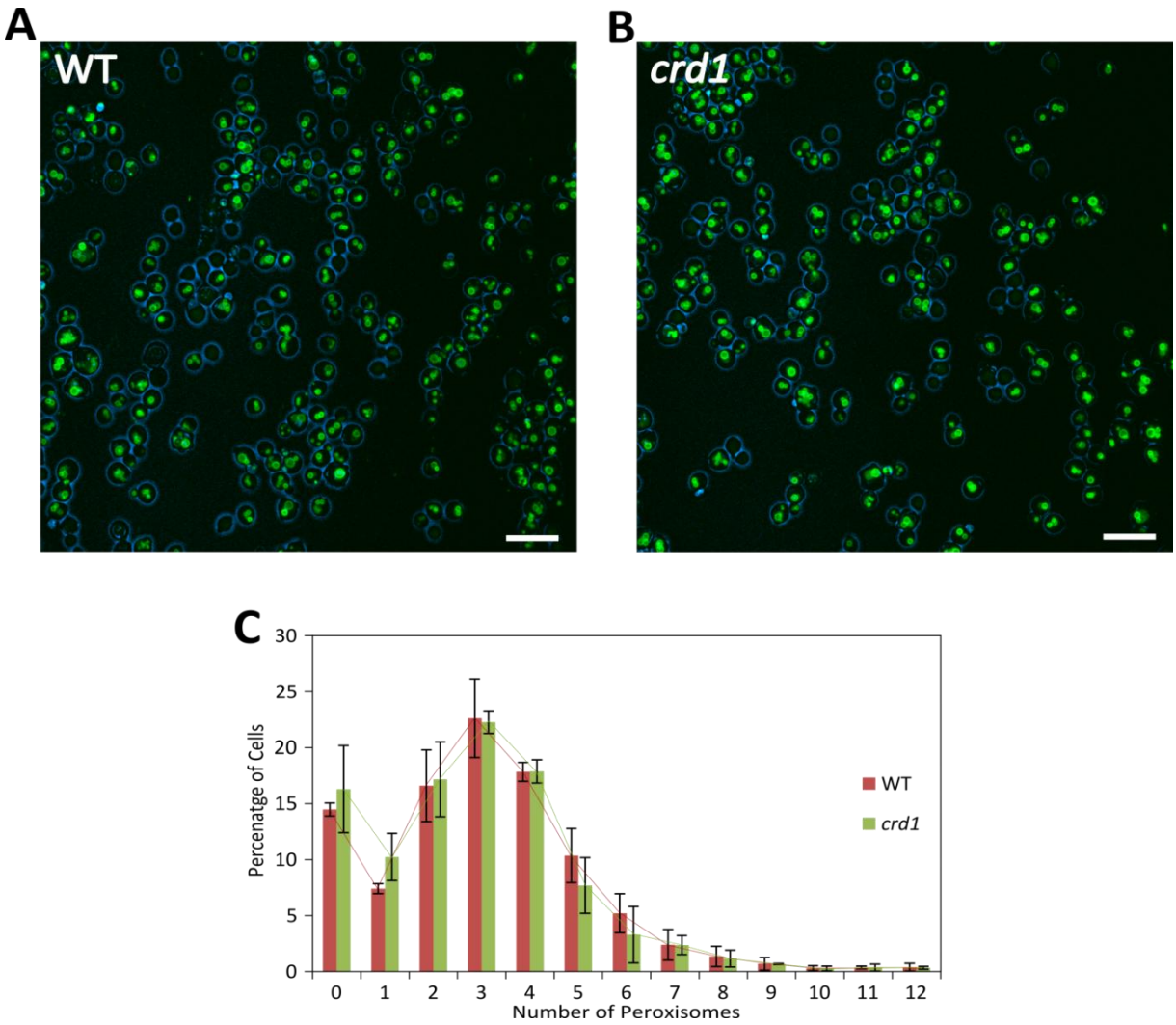

Figure 7. FM analysis of chemostat grown WT and *crd1* cells. WT and *crd1* cells expressing PMP47-mGFP and GFP-SKL were grown in methanol limited chemostat. Fluorescence images of WT **(A)** and *crd1* cells **(B).** Peroxisome distribution in WT and *crd1* cells **(C)**. The above images shown are representative image of WT and *crd1* cells. Data represent average number of peroxisomes ± standard deviation obtained from 2 different time points for WT and *crd1* strain.The scale bar represents 5 µm.

PE depletion reduces the peroxisome number in *S. cerevisiae*

To investigate the effect of PE depletion on peroxisomes in *S. cerevisiae*, PE synthesis was disturbed by deleting the genes from three different PE synthesis pathways. Deletion of *PSD1*, *PSD2* and *CKI1 EKI1 DPL1* did not result in drastic growth defect in medium containing 0.5% glucose (non-inducing condition) (**Fig. 9A**). However, *PSD1* deletion resulted in a

severe growth defect in the medium containing 0.1% glucose and 0.1% oleate (peroxisome inducing condition) (**Fig. 9B**).

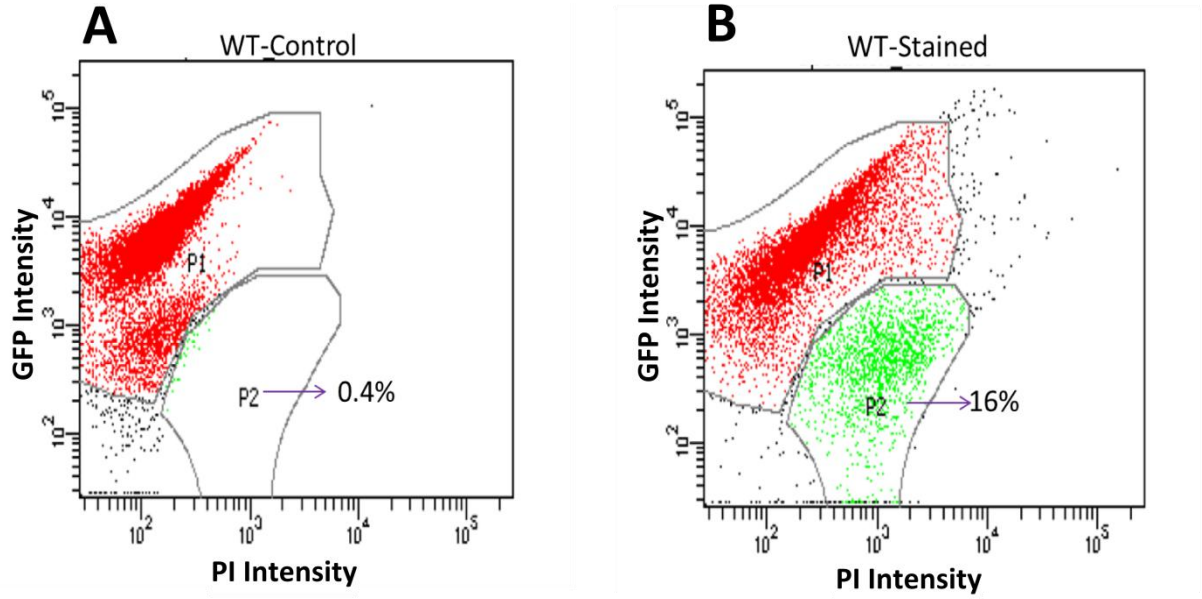

Figure 8. Viability staining for WT cells. Distribution of cell population in WT-non stained (control) and WT-stained cells based on GFP intensity **(A)** and GFP intensity/PI staining **(B)**. Y-axis represents the intensity of GFP signal. X-axis represents the PI stain intensity.

Maximum OD reached by *psd1*, *psd2* and *cki1 eki1 dpl1* cells was significantly lower than the WT cells in the inducing as well as in the non-inducing condition (**Table. S1**). This was accompanied by significantly longer doubling time for *psd1* and *psd2* cells in both the conditions (**Table. S1**). However *cki1 eki1 dpl1* cells had longer doubling time only in peroxisome inducing condition.

To study the effect of *PSD1*, *PSD2* and *CKI1 EKI1 DPL1* deletion on peroxisome numbers, WT, *psd1*, *psd2* and *cki1 eki1 dpl1* cells having peroxisomal marker GFP-SKL under the P_{MET25} promoter were grown in medium containing 0.5% glucose for 16 hours or 0.1% glucose and 0.1% oleate medium for 24 hours. Due to severe growth defect, *psd1* cells were also analyzed at 45 hours (the time they reach equal OD as WT cells). Subsequent fluorescence microscopy analysis revealed the presence of bigger and more intense GFP spots in *psd1* cells when compared to WT cells (**Fig. 10B and Supplementary Fig. 1B**).

Peroxisome quantification revealed that the average number of peroxisomes in *psd1* cells was reduced when compared to the WT cells (**Table. 4**).

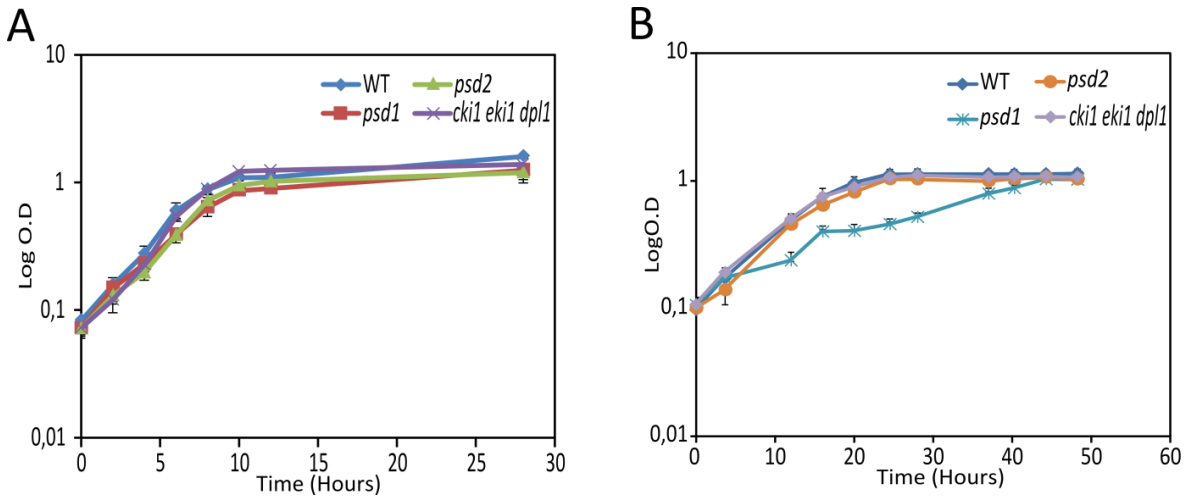

Figure 9. Growth properties of *S. cerevisiae* WT, *psd1*, *psd2* and *cki1 eki1 dpl1* cells. WT , *psd1*, *psd2* and *cki1 eki1 dpl1* cells were grown in medium containing 0.5% glucose **(A)** and 0.1% glucose/0.1% oleate **(B).** The optical density was measured at 600 nm. Data represent mean ± standard deviation from 2 independent cultures.

Analysis of the distribution of peroxisomes in the *psd1* cells clearly showed increased number of cells with one and two peroxisomes when compared to WT cells (**Fig. 10E**). Furthermore, exponentially growing *psd1* cells were examined under the microscope to check for drastic phenotype. Exponentially growing *psd1* cells were not able to import GFP-SKL (**Supplementary Fig. 10B**). More than 50% of cells had strong cytosolic GFP signal. In contrast to *psd1*, GFP spots in *psd2* and *cki1 eki1 dpl1* cells were similar to that of WT cells (**Fig. 10CD**). Quantification of peroxisome in *psd2* and *cki1 eki1 dpl1* cells grown on 0.5% glucose revealed no difference relative to the WT in neither the average number of peroxisomes per cell nor in the distribution of peroxisomes number in the population of cells (**Fig. 10FG**).

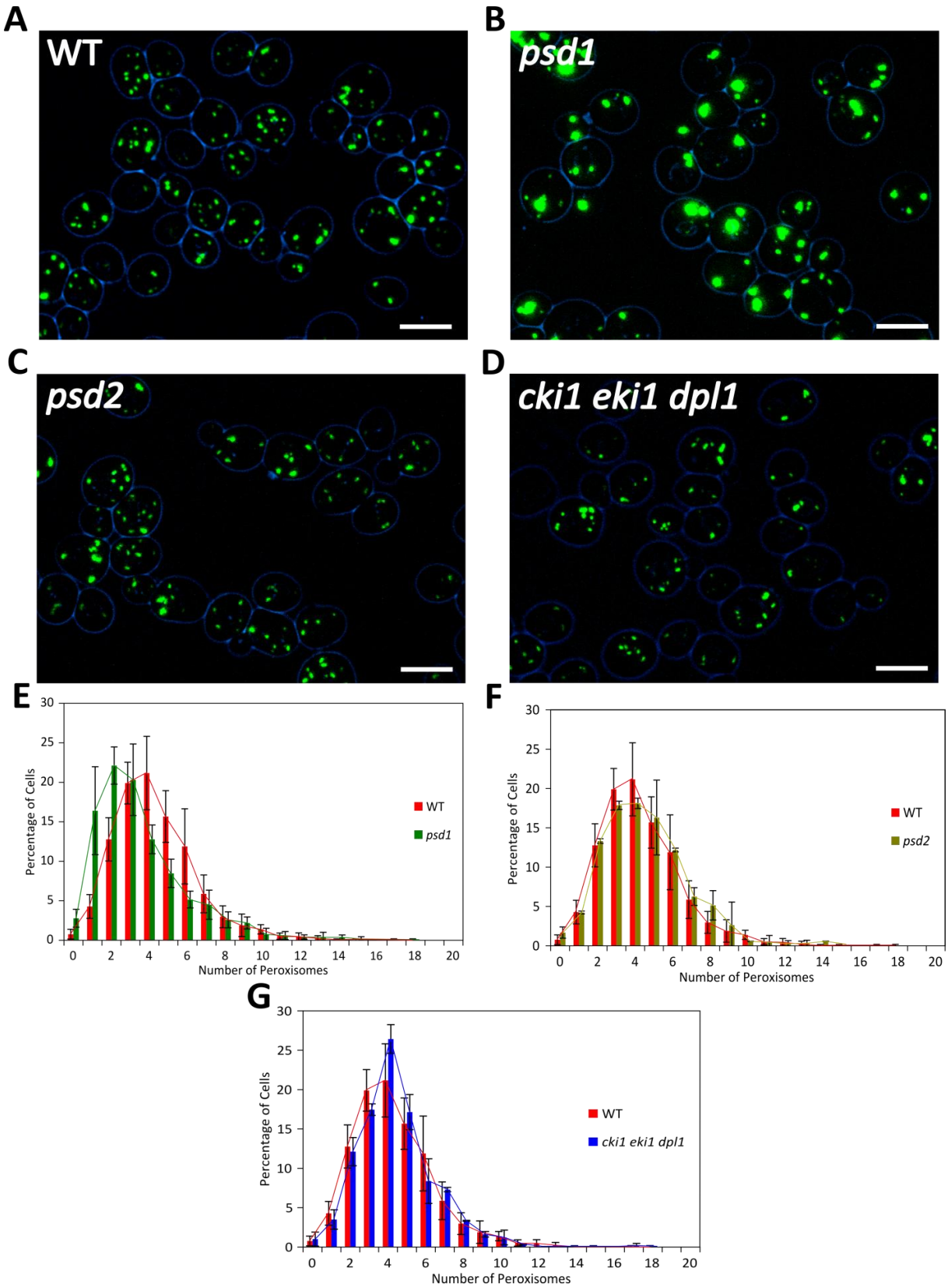

Figure 10. FM analysis of *S. cerevisiae* WT, *psd1*, *psd2* and *cki1 eki1 dpl1* cells. WT, *psd1*, *psd2* and *cki1 eki1 dpl1* cells expressing GFP-SKL were grown for 16 hours on medium containing 0.5% glucose. Fluorescence images of WT **(A)**, *psd1***(B)**, *psd2***(C)**, *cki1 eki1 dpl1***(D)** cells**.** Peroxisome distribution *psd1***(E)**, *psd2***(F)**, *cki1 eki1 dpl1* cells **(G)** compared with WT. Data represent average number of peroxisomes ± standard deviation from 7 independent WT, 4 independent *psd1* and *psd2* and 2 independent *cki1 eki1 dpl1* cultures.The scale bar represents 5 µm.

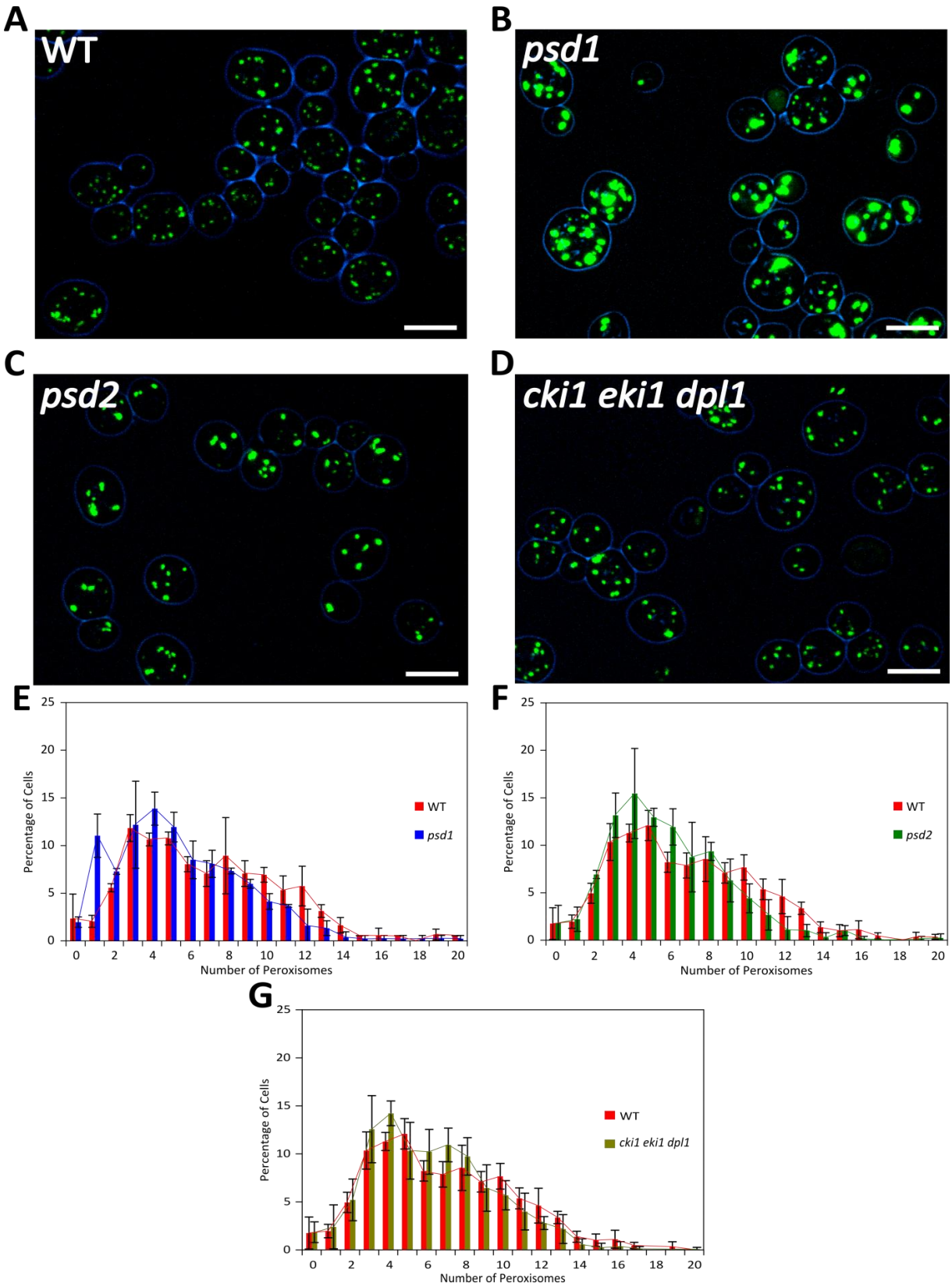

Figure 11. FM analysis of *S. cerevisiae* WT, *psd1*, *psd2* and *cki1 eki1 dpl1* cells. WT, *psd1*, *psd2* and *cki1 eki1 dpl1* cells expressing GFP-SKL were grown for 24 hours on medium containing 0.1% glucose/0.1% oleate. Fluorescence images of WT **(A)**, *psd1***(B)**, *psd2***(C)**, *cki1 eki1 dpl1***(D)** cells**.** Peroxisome distribution *psd1***(E)**, *psd2***(F)**, *cki1 eki1 dpl1* cells **(G)** compared with WT. Data represent average number of peroxisomes ± standard deviation from 4 independent WT and 2 independent *psd1*, *psd2* and *cki1 eki1 dpl1* cultures. Scale bar : **(A-D)**5 µm.

Table 4. Peroxisome quantification of *S. cerevisiae* WT, *crd1*, *psd1*, *psd2* and *cki1 eki1 dpl1* cells

Growth conditions	Strain	Average number of peroxisomes per cell	Repeats
0.5% Glucose (16 Hours)	WT	4,4	7 (200-330 cells)
	crd1	4,5	5 (200-340 cells)
	psd1	3,5	4 (160-390 cells)
	psd2	4,5	4 (180-200 cells)
	cki1 eki1 dpl1	4,3	2 (270-370 cells)
0.1% Glucose & 0.1% oleate (24 Hours)	WT	7,0	4 (190-360 cells)
	crd1	7,6	4 (160-350 cells)
	psd1	5,5	2 (210-260 cells)
	psd2	5,8	2 (140-230 cells)
	cki1 eki1 dpl1	6,2	2 (190-280 cells)
0.1% Glucose & 0.1% oleate (45 Hours)	WT	7,1	2 (280-345 cells)
	psd1	4,9	2 (190-220 cells)

Since *psd1* cells had severe growth defect while growing in medium containing 0.1% glucose and 0.1% oleate we quantified peroxisome numbers at same time point as well as at same OD. Peroxisome quantification at the same time point (24 hours) and upon reaching similar OD (45 Hours) revealed reduced average peroxisomes number in *psd1* cells relative to WT cells (**Table. 4**).

Analysis of the peroxisome distribution also showed higher percentage of cells with one and two peroxisomes (**Fig. 11E and Supplementary Fig. 2**). Unlike for *psd1* cells, intensity of GFP spots was not altered in *psd2* and *cki1 eki1 dpl1* cells when compared with WT cells (**Fig. 11CD**). Peroxisome quantification in *psd2* cells showed reduced average number of peroxisomes per cell (**Table. 4**). Average number of peroxisomes per cell was also slightly reduced in *cki1 eki1 dpl1* cells when compared with WT cells (**Table. 4**). Interestingly, in both *psd2* and *cki1 eki1 dpl1* cells we observed more number of cells having 2 and 3 peroxisomes in the peroxisome distribution when compared to WT cells (**Fig. 11FG**). Altogether, these data suggest that depletion of PE by deleting genes involved in three different pathways results in reduced number of peroxisomes in *S. cerevisiae*.

PE depletion does not affect the peroxisomes number in *H. polymorpha*

To study the effect of PE depletion on other yeast *PSD1* and *PSD2* homologues were deleted in the methylotrophic yeast *H. polymorpha*. *psd1* cells had severe growth defect in the medium containing 0.5% (glucose non-inducing condition) and 0.5% methanol (peroxisome inducing conditions) (**Fig. 12AB**).

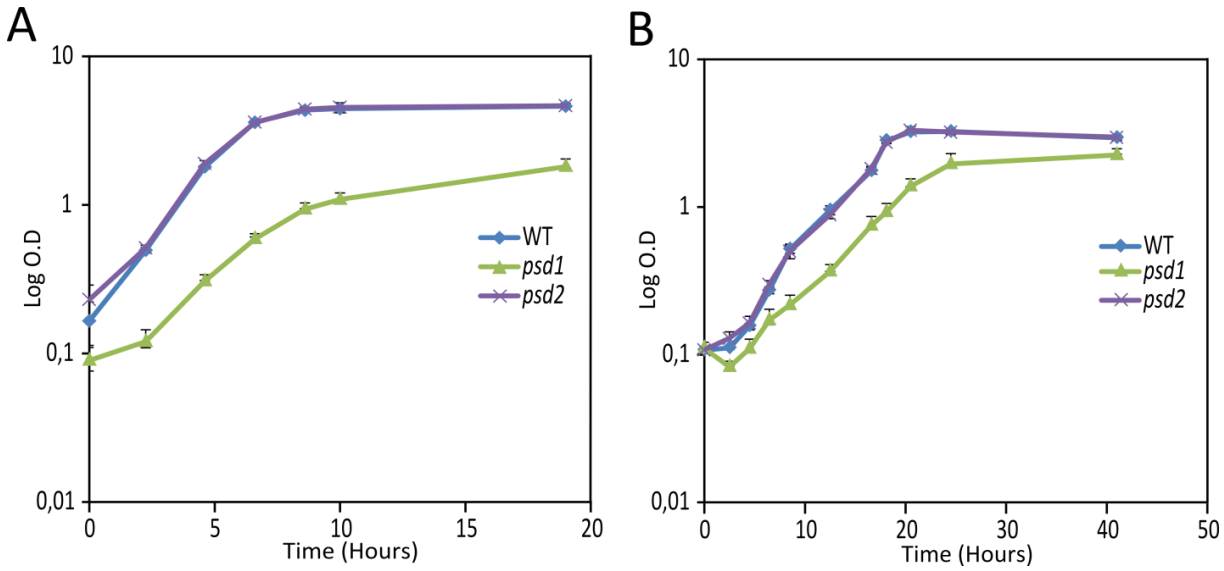

Figure 12. Growth properties of *H. polymorpha* WT, *psd1* and *psd2* cells. WT , *psd1* and *psd2* cells were grown in medium containing 0.5% glucose **(A)** and 0.5% methanol **(B).** The optical density was measured at 600 nm. Data represent mean ± standard deviation from 2 independent cultures.

The deletion of *PSD2* did not result in growth defect (**Table. S2**) Maximum OD reached by the *psd1* cells was lower than WT cells in both the conditions (**Table. S2**). Doubling time for *psd1* cells was significantly longer than WT cells in both the conditions. To avoid the influence of growth difference on peroxisome quantification, WT and *psd1* cells having PMP47-mGFP were grown in methanol limited chemostats at equal dilution rate (D=0.1).

WT and *psd1* cells expressing two peroxisomal markers Pmp47-mGFP/ GFP-SKL were grown in methanol limited chemostats. FM analysis and peroxisome quantification showed no difference in the average number of peroxisomes in *psd1* cells when compared with WT cells (**Table. 5**). Similar peroxisome distribution was observed in *psd1* cells when compared to WT cells (**Fig. 13C**). Since *psd2* cells did not display any growth defects, they were grown in flasks containing 0.5% methanol for 24 hours.

Table 5. Peroxisome quantification of *H. polymorpha* WT, *crd1*, *psd1* and *psd2* cells

Experimental Setup	Strain	Average number of peroxisomes per cell
Chemostat 1	WT	3,0
	crd1	2,9
Chemostat 1	WT	2,9
	psd1	3,2
Batch culture	WT	3,8
	psd2	3,8

Data from peroxisome quantifications represents average number of peroxisomes for chemostats at two different time points and two independent batch cultures. About 800 to 1200 cells were analyzed for each quantification

FM analysis and peroxisome quantification clearly showed that there is no significant difference in the average number of peroxisomes per cell and peroxisome distribution when compared to WT cells (**Table. 5** and **Fig. 14C**). These data clearly shows that depletion of PE by deleting *PSD1* and *PSD2* in *H. polymorpha* does not have any drastic effect on the number of peroxisomes.

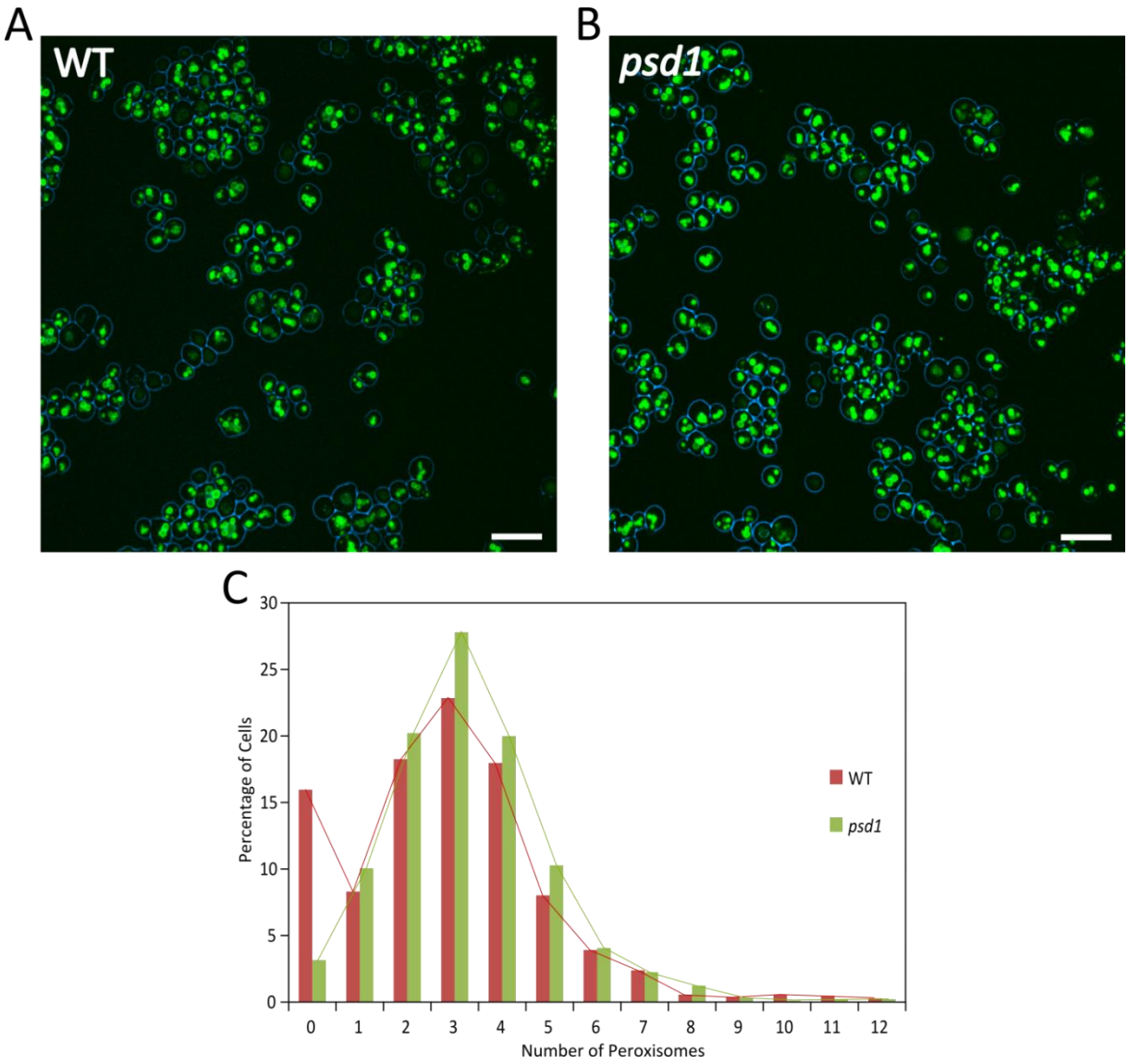

Figure 13. FM analysis of chemostat grown WT and *psd1* cells. WT and *psd1* cells expressing PMP47-mGFP and GFP-SKL were grown in methanol limited chemostat. Fluorescence images of WT **(A)** and *psd1* cells **(B).** Peroxisome distribution in WT and *psd1* cells **(C)**. The above images shown are representative image of WT and *psd1* cells. Data represent average number of peroxisomes from a chemostat.The scale bar represents 5 µm.

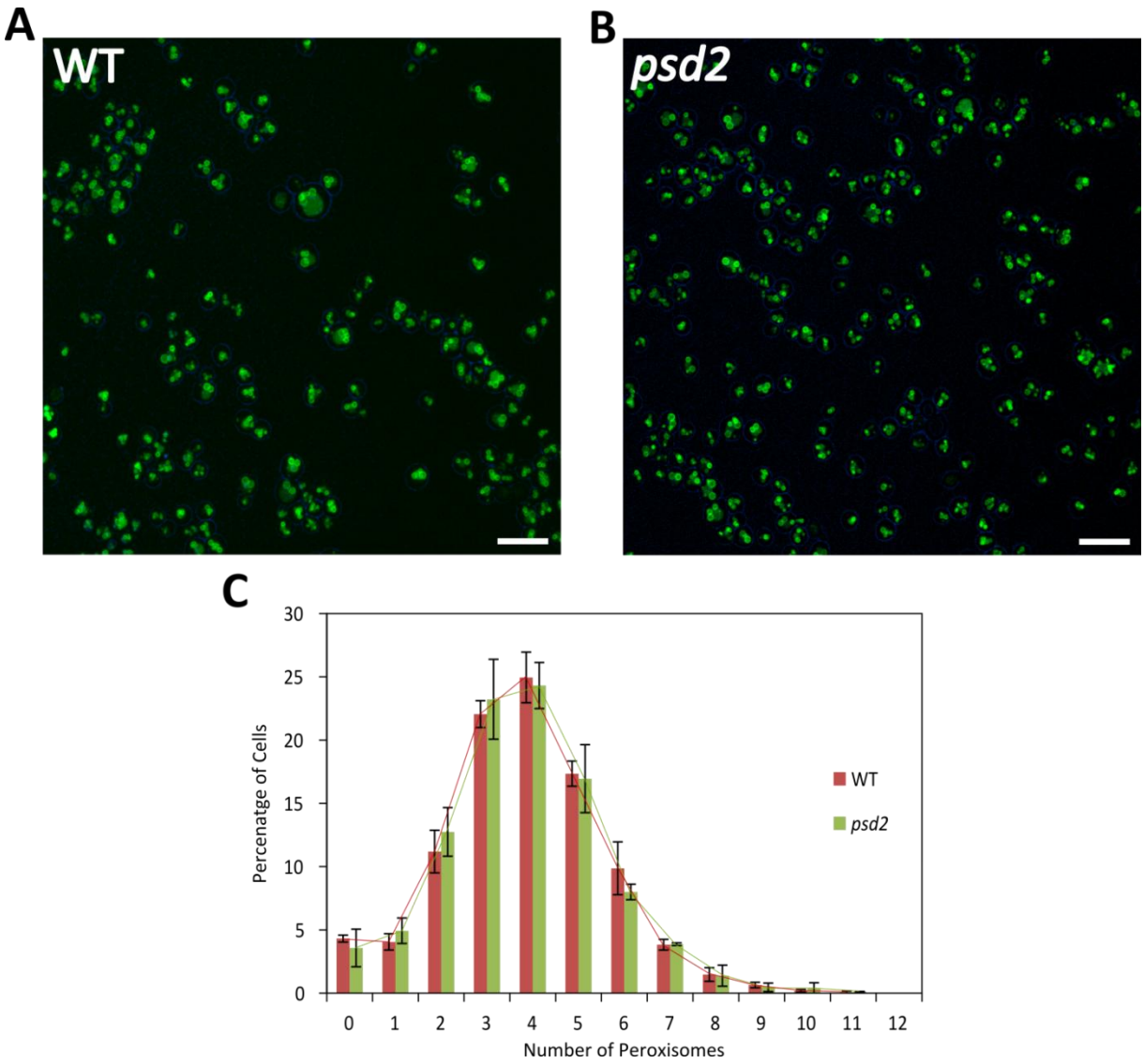

Figure 14. FM analysis of batch flask grown WT and *psd2* cells. WT and *psd2* cells expressing PMP47-mGFP and GFP-SKL were grown for 24 hours in the medium containing 0.5% methanol. Fluorescence images of WT **(A)** and *psd2* cells **(B).** Peroxisome distribution in WT and *psd2* cells **(C)**. The above images shown are representative image of WT and *psd2* cells. Data represent average number of peroxisomes ± standard deviation from 2 independent WT and *psd2* cultures.The scale bar represents 5 µm.

Discussion

Cardiolipin is a special phospholipid localized to mitochondria. Presence of cardiolipin in peroxisomal membrane and its putative function is highly speculated [40]. Studies in yeast indicated presence of that phospholipid in the peroxisomal fraction, however its role at that location has not been elucidated [36, 40]. Here we studied the effect of CL deficiency on peroxisome abundance by deleting *CRD1* gene in *S. cerevisiae* and *H. polymorpha*.

Surprisingly, peroxisome quantifications did not reveal any drastic phenotype in the *crd1* strain of *S. cerevisiae* and *H. polymorpha*. Previous studies have shown that CL consists of less than 7% of the total phospholipids in the peroxisomal membrane. Recently it has been shown that peroxisomes are juxtaposed to mitochondria at specific mitochondrial domains suggesting tight association between these 2 organelles [96]. It is therefore possible that CL is not present in the peroxisomes and the presence of CL in the peroxisomal fraction reported so far might be an artifact of mitochondrial membrane contamination during organelle isolation.

Alternatively, the functions of CL may be compensated by other phospholipids, including PE. It has been shown that mitochondrial phenotypes occurring in *crd1* strain of *S. cerevisiae* are compensated by PE [49, 55]. Remarkably, strains deficient in both CL and PE are not viable suggesting partial overlapping functions of these phospholipids [49]. Surprisingly, in peroxisomes inducing conditions, slightly increased number of peroxisomes in *crd1* cells of *S. cerevisiae* was observed. This might be due to secondary effect of CL deficiency, like altered phospholipid metabolism or induction of the retrograde response.

PE is a cone shaped phospholipid required for vesicle formation, membrane fusion and maintaining mitochondrial morphology [49]. Events involving membrane fusion are also thought to be involved in peroxisome biogenesis. For instance last step of peroxisomal fission in *S. cerevisiae* involves the Vps1/Dnm1 dependent division and separation of small organelle. Furthermore, vesicles carriers containing lipids and certain PMPs have to fuse with peroxisomes to deliver its contents.In yeast, PE is synthesized by three pathways at distinct cellular locations. Remarkably, only the *PSD1* deletion reduced the peroxisome number in the cells in both peroxisome inducing conditions and non-inducing condition. The result is not surprising as Psd1 has been shown to responsible for 80% of the total cellular Psd activity [62]. Notably, the intensity of fluorescent spots in *psd1* cells producing GFP from P_{MET25} promoter was higher than in WT cells.The GFP intensity was also slightly increased in *crd1 S.*

cerevisiae cells, pointing to non-specific mechanism, likely to be associated with mitochondrial function. The nature of that induction remains unclear, however we speculate that it might be related to the disturbance of the sulphur containing amino acid biosynthetic pathways and a transcriptional response. The higher GFP intensity in *psd1* cells is unlikely to affect the results of peroxisome quantification as *S. cerevisiae* peroxisomes are rarely clustering and thus the chance of 2 organelles in close proximity to each other counted as one GFP spot is low. To completely rule out this possibility, another promoter for GFP-SKL expression could be used or peroxisome abundance should be analyzed by electron microscopy. The EM analysis would also provide information about the morphology and size of the organelles.

Previous studies have shown that PE produced through Kennedy pathway and Psd2 is only a minor fraction of total PE present [62]. Interestingly, *psd2* cells of *S. cerevisiae* had normal GFP spots, but reduced peroxisome numbers in peroxisome inducing conditions. *cki1 eki1 dpl1* cells of *S. cerevisiae* also had normal GFP spots, but slightly reduced peroxisome numbers in peroxisome inducing conditions. We speculate that either PE synthesized through three different pathways are not the same or the efficiency and the spatial separation of the enzymes present in the three different pathways might be responsible for the observed phenotype. The PE synthesized might have different fatty acid side chains and might contribute differently to the peroxisomes due to spatial separation. Furthermore, PE is converted to PC by two methylating enzymes, so it is important to consider that the phenotype observed in all the three strains of *S. cerevisiae* might be also due depletion of PC. Analysis of *psd1 psd2* strain supplied with external choline to avoid PC depletion would dissect the effect of PE depletion alone on peroxisome abundance. Previously, Rosenberger et al studied all these three PE mutants in *S. cerevisiae* and found smaller peroxisomes in *psd1* cells [41]. However, reduced peroxisome abundance after depleting PE was not observed. It has to be

taken into account that the medium used in both the case are different which might the reason for not observing reduced peroxisome numbers in these mutant strains. The relationship between impaired PE production and reduced peroxisome numbers remains highly speculative. PE was shown to be involved in mitochondrial fission and fusion processes [49]. Presence of PE is important for formation of non-lamellar lipid structure during fission process. We speculate that the reduced number of peroxisomes might be due to a partial inhibition of the peroxisomal fission machinery. Since the GFP spots in the FM images of *psd1* cells were too intense, we couldn't conclude anything regarding the size of the peroxisomes. If they happen to be bigger then, the hypothesis of partial fission block can be proved by depleting PE in *pex*11 or *dnm*1 strains.

In contrast to these results *psd1* and *psd2* cells of *H. polymorpha* did not have any effect on peroxisome number. Fast growth of *H. polymorpha* in mineral medium requires addition of 0.05% yeast extract. We speculate that this component might contain small amounts of ethanolamine and choline and this might be the reason for not observing an effect of PE depletion in these *H. polymorpha* strains.

Overall, our studies indicate that PE depletion may reduce peroxisome abundance in yeast. Further studies should focus on how this phospholipids is transported to the organelle and how does it contribute to the organelle biogenesis.

Supplementary data.

Table S1. Maximum optical density and Doubling time of *S. cerevisiae* WT, *crd1*, *psd1*, *psd2* and *cki1 eki1 dpl1* cells

Growth conditions	Strain	Maximum optical density	Doubling time (Hours)
0.5% Glucose	WT	1,59 ± 0,05	2,07 ± 0,06
	crd1	1,22 ± 0,13	1,27 ± 0,06
	psd1	1,17 ± 0,12	2,91 ± 0,44
	psd2	1,12 ± 0,20	2,56 ± 0,52
	cki1 eki1 dpl1	1,30 ± 0,08	1,85 ± 0,00
0.1% Glucose & 0.1% oleate	WT	1,21 ± 0,02	7,99 ± 0,32
	crd1	1,34 ± 0,04	7,47 ± 0,49
	psd1	1,10 ± 0,01	15,73 ± 0,12
	psd2	1,10 ± 0,04	9,54 ± 0,21
	cki1 eki1 dpl1	1,14 ± 0,01	9,68 ± 1,32

Table S2. Maximum optical density and Doubling time of *H. polymorpha* WT, *crd1*, *psd1* and *psd2* cells

Growth conditions	Strain	Maximum optical density	Doubling time (Hours)
0.5% Glucose	WT	4,61 ± 0,01	1,52 ± 0,03
	crd1	4,10 ± 0,13	1,42 ± 0,05
	psd1	1,91 ± 0,12	1,89 ± 0,19
	psd2	4,68 ± 0,21	1,55 ± 0,20
0.5% Methanol	WT	3,35 ± 0,04	3,94 ± 0,08
	crd1	2,50 ± 0,11	3,88 ± 0,21
	psd1	2,38 ± 0,10	4,62 ± 0,50
	psd2	3,26 ± 0,09	3,91 ± 0,23

Table S3. Plasmids used in this study

Plasmid	Description	Reference
pDONR-P4-P1R	Standard Gateway vector	Invitrogen
pDONR-P2R-P3	Standard Gateway vector	Invitrogen
pENTR_41_5'CRD1	pDONR-P4-P1R containing 5' region of *CRD1*, kan^R	This study
pENTR_23_3'CRD1	pDONR-P2R-P3 containing 3' region of *CRD1*, kan^R	This study
pENTR_41_5'PSD1	pDONR-P4-P1R containing 5' region of *PSD1*, kan^R	This study
pENTR_23_3'PSD1	pDONR-P2R-P3 containing 3' region of *PSD1*, kan^R	This study
pENTR_41_5'PSD2	pDONR-P4-P1R containing 5' region of *PSD2*, kan^R	This study
pENTR_23_3'PSD2	pDONR-P2R-P3 containing 3' region of *PSD2*, kan^R	This study
pENTR-221-HPH	pENTR-221 containing hygromycin marker, kan^R	[97]
pDEST-R4-R3-NAT	pDEST-R4-R3 containing nourseothricin marker, amp^R	[98]
pDEST_NAT_CRD1_DEL_HPH	pDEST-R4-R3 containing *CRD1* deletion cassette with hygromycin marker, amp^R	This study
pDEST_NAT_PSD1_DEL_HPH	pDEST-R4-R3 containing *PSD1* deletion cassette with hygromycin marker, amp^R	This study
pDEST_NAT_PSD2_DEL_HPH	pDEST-R4-R3 containing *PSD2* deletion cassette with hygromycin marker, amp^R	This study
pENTR_221_NAT	pENTR-221 containing nourseothricin marker, kan^R	[97]
pUG6	pUG6 containing gentamicin resistance marker	[99]
pHIPX7	pHIP containing eGFP-SKL under the control of P_{TEF1}; leucine marker; kan^R	[100]
pMCE7	Plasmid containing PMP47-mGFP under the control of endogenous promoter	[101]

Table S4. Primers used for cloning *S. cerevisiae* strains in this study

Primer name	Sequence
ScCRD1_selF	ATCATTGTGCGGCGACTATT
ScCRD1_selR	GCGTCTGAATGTGTTAAATCCA
ScPSD1_del_F	GCCAGTTAAGAACGCCTTGGCGCAAGGGAGGACGCTCCTCATGGGGAGGAC AGCTGAAGCTTCGTACGC
Sc_PSD1_del_R	CAGGTATGTGGTTCCAAGTGTTTGTCGCTCTTTGAATTTGTCACAAATTCGCA TAGGCCACTAGTGGATCTG
ScPSD1_selF	CCAGCACCTTTTTGGTGTTT
ScPSD1_selR	AAGGGGTACATGACATGGCTA
ScPSD2_del_F	GTATCAATTGGTAAAGAATCCTCGATTTTCAGGAGCATCCAACGACGAAGCC CACACACCATAGCTTCAA
ScPSD2_del_R	TACTCATCCCGACTTTGACTAACGTTTCAATGCGTTCTGAAGAGTTTTTCACG TTTTCGACACTGGATGG
ScPSD2_selF	GCCCTAACGCATGTGCTACT
ScPSD2_selR	TTCCTGGTATGAAACCATTGC
ScEKI1_del_F	TACGAAAGTAGTAGCAGAAATTAACAGATACAGATCTGCAATTTGGCATAC AGCTGAAGCTTCGTACGC
Sc_EKI1_del_R	TAACTCCCAATGTAATTAAATCGCCCCAAAAGACAGACATTTTTTCTTTACG CATAGGCCACTAGTGGATCTG
ScEKI1_selF	GGCCACTAGACAGCATGTGA
ScEKI1_selR	TCCATTGACCTAACATGTTGAAA
ScCKI1_del_F	ACTGATGTCACAGATAGTTTGGGTTCGACTTCGTCGGAATATATTGAGATTC CCACACACCATAGCTTCAA
ScCKI1_del_R	GAACTTGAAAGAGCTGAAATTTTTGCATTCTTCTTCGGTGATTATGCCTAAC GTTTTCGACACTGGATGG
ScCKI1_selF	GCTCTGTGGCTGTAAGTAAGGA
ScCKI1_selR	GCTTTATTTCCTTGGCCTTTG
ScDPL1_del_F	TACCGAGCAAGTAGGCTAGCTTCTGTAAAGGGATTTTTCCATCTAATACACC CACACACCATAGCTTCAA
ScDPL1_del_R	ACATTGCACTCTCGTTCTTTAAATTATGTATGAGATTTGATTCTATATAGCGT TTTCGACACTGGATGG
ScDPL1_selF	TGCCTATCGTTTATCGCCTTA
ScDPL1_selR	CTTTCTCATCCCCTCGTGAA
KanC	TGATTTTGATGACGAGCGTAAT
KanB	CTGCAGCGAGGAGCCGTAAT

Table S5. Primers used for cloning *H.polymorpha* strains in this study

Primer name	Sequence
CRD1_OL_F	GAAATATTTTTTGTTGAGAATAGCTCATCAGGGCTGGTATTG
CRD1_OL_R	CAATACCAGCCCTGATGAGCTATTCTCAACAAAAAATATTTC
CRD1_del5F	GGGGACAACTTTGTATAGAAAAGTTGTTTCTCGAGGAGAGTAGGGTTG
CRD1_del5R	GGGGACTGCTTTTTTGTACAAACTTGCCCGGCCAGTAGCAGCATTA
CRD_del3F	GGGGACAGCTTTCTTGTACAAAGTGGTAATTGGGACTTCTCGCTCATC
CRD_del3R	GGGGACAACTTTGTATAATAAAGTTGTAGAATGTCACGCAGCCAACT
CRD1_del_F	TCTCGAGGAGAGTAGGGTTG
CRD1_del_R	AGAATGTCACGCAGCCAACT
CRD1_sel5_F	GCATCGTGTTCTTTCAGCAC
CRD1_sel3_R	ACCGCAGACCTAGTGGAAGA
CRD1_TGA_F	CATGGAAATATTTTTTGTTGAGAATAG
PSD1_del5F	GGGGACAACTTTGTATAGAAAAGTTGTTAACGAAAACTGGTGGCAAAG
PSD1_del5R	GGGGACTGCTTTTTTGTACAAACTTGCGAAGTCAACGTGAACCACGA
PSD1_del3F	GGGGACAGCTTTCTTGTACAAAGTGGTAACACTTGTCGGCGCTGAAG
PSD1_del3R	GGGGACAACTTTGTATAATAAAGTTGTCAGTGAGCAGAGCTTGATGG
PSD1_del_F	AACGAAAACTGGTGGCAAAG
PSD1_del_R	CAGTGAGCAGAGCTTGATGG
PSD1_sel5_F	GACACTGTGGTCGAAAGCAA
PSD1_sel3_R	GCTGAATTCCACGGTGCTA
PSD2_del5F	GGGGACAACTTTGTATAGAAAAGTTGTTGCGATAATAGAGTGACGAGAGGA
PSD2_del5R	GGGGACTGCTTTTTTGTACAAACTTGCGGTCTGCGACACTGAAGGTT
PSD2_del3F	GGGGACAGCTTTCTTGTACAAAGTGGTAGCAGATTGTCGATGCTGTGT
PSD2_del3R	GGGGACAACTTTGTATAATAAAGTTGTCGTGCCTGTTGCTGCTACTA
PSD2_del_F	GCGATAATAGAGTGACGAGAGGA

PSD2_del_R	CGTGCCTGTTGCTGCTACTA
PSD2_sel5_F	CATTGAGTGGTTTCGGGTTT
PSD2_sel3_R	GTAAAGCTGCGGTTCTTTCG
Universal primer 27	GGGTGTTTTGAAGTGGTACG
Universal primer 28	TCATCTGCCCAGATGCGAAG

Supplementary Figure 1.

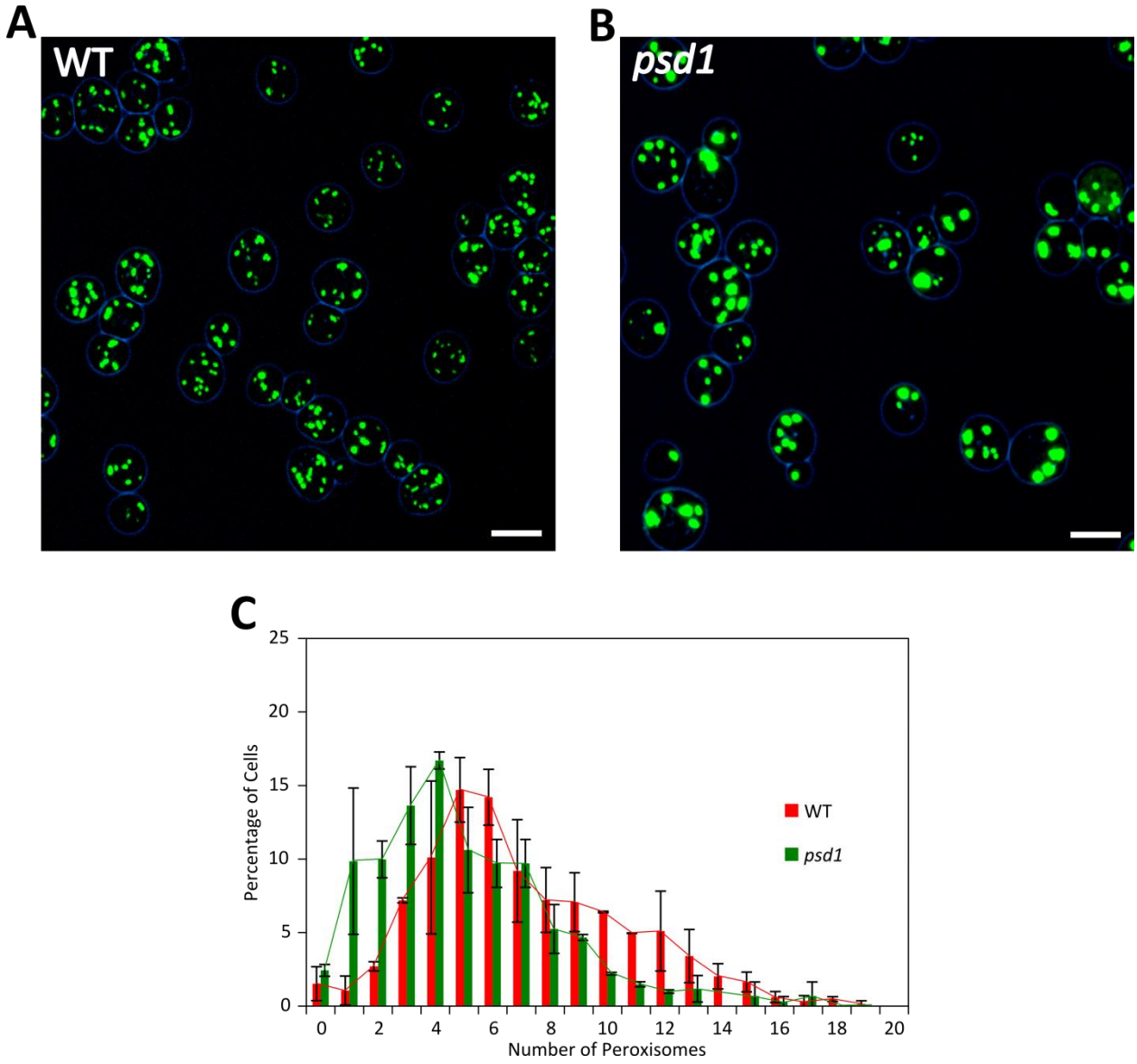

SupplementaryFigure 1. FM analysis of *S. cerevisiae* WT and *psd1* cells. WT and *psd1* cells expressing GFP-SKL were grown for 45 hours in the medium containing 0.1% glucose/0.1% oleate. Fluorescence images of WT **(A)** and *psd1* cells **(B).** Peroxisome distribution in WT and *psd1* cells **(D)**. The above images shown are representative image of WT and *psd1* cells. Data represent mean from 2 independent WT and *psd1* cultures.The scale bar represents 5 µm.

Supplementary Figure 2.

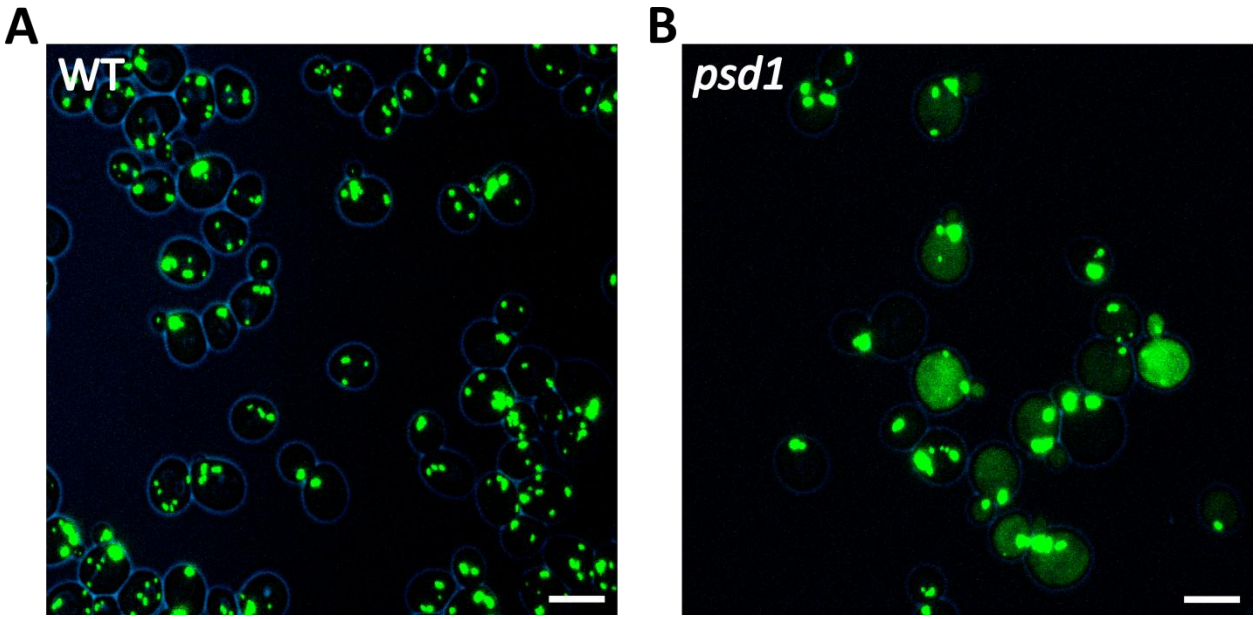

SupplementaryFigure 2. FM analysis of *S. cerevisiae* WT and *psd1* cells. WT and *psd1* cells expressing GFP-SKL were grown for 7 hours in the medium containing 0.5% glucose. Fluorescence images of WT **(A)** and *psd1* cells **(B).** Fluorescence image of *psd1* cells showing cytosolic GFP in exponentially growing cells. The above images shown are representative image of WT and *psd1* cells. More than 50% *psd1* cells had cytosolic GFP.The scale bar represents 5 µm.

1. Schlüter A, Fourcade S, Ripp R, Mandel JL, Poch O, Pujol A: **The evolutionary origin of peroxisomes: an ER-peroxisome Connection**. *Mol Biol Evol* 2006, **23**:838–845.

2. Van den Bosch H, Schutgens RBH, Wanders RJA, Tager JM: **Biochemistry of peroxisomes**. *Annu Rev Biochem* 1992, **61**:157–197.

3. Muller WH, van der Krift TP, Krouwer AJ, Wosten HA, van der Voort LH, Smaal EB, Verkleij AJ: **Localization of the pathway of the penicillin biosynthesis in *Penicillium chrysogenum*.***EMBO J* 1991, **10**:489–495.

4. Liu F, Ng SK, Lu Y, Low W, Lai J, Jedd G: **Making two organelles from one: Woronin body biogenesis by peroxisomal protein sorting**. *J Cell Biol* 2008, **180**:325–339.

5. Reumann S, Weber APM: **Plant peroxisomes respire in the light: Some gaps of the photorespiratory C2 cycle have become filled—Others remain**. *Biochim Biophys Acta BBA - Mol Cell Res* 2006, **1763**:1496–1510. [*Peroxisomes: Morphology, Function, Biogenesis and Disorders*]

6. Wanders RJA, Waterham HR: **Biochemistry of mammalian peroxisomes revisited**. *Annu Rev Biochem* 2006, **75**:295–332.

7. Dixit E, Boulant S, Zhang Y, Lee ASY, Odendall C, Shum B, Hacohen N, Chen ZJ, Whelan SP, Fransen M, Nibert ML, Superti-Furga G, Kagan JC: **Peroxisomes are signaling platforms for antiviral innate immunity**. *Cell* 2010, **141**:668–681.

8. Wanders RJA: **Peroxisomes, lipid metabolism, and peroxisomal disorders**. *Mol Genet Metab* 2004, **83**:16–27. [*ASHG 2004 Meeting Toronto*]

9. Kim PK, Mullen RT, Schumann U, Lippincott-Schwartz J: **The origin and maintenance of mammalian peroxisomes involves a de novo PEX16-dependent pathway from the ER**. *J Cell Biol* 2006, **173**:521–532.

10. Hettema EH, Erdmann R, van der Klei I, Veenhuis M: **Evolving models for peroxisome biogenesis**. *Curr Opin Cell Biol* 2014, **29**:25–30. [*Cell Organelles*]

11. Van der Zand A, Gent J, Braakman I, Tabak HF: **Biochemically distinct vesicles from the endoplasmic reticulum fuse to form peroxisomes**. *Cell* 2012, **149**:397–409.

12. Motley AM, Hettema EH: **Yeast peroxisomes multiply by growth and division**. *J Cell Biol* 2007, **178**:399–410.

13. Brocard C, Hartig A: **Peroxisome targeting signal 1: Is it really a simple tripeptide?***Biochim Biophys Acta BBA - Mol Cell Res* 2006, **1763**:1565–1573. [*Peroxisomes: Morphology, Function, Biogenesis and Disorders*]

14. Swinkels BW, Gould SJ, Bodnar AG, Rachubinski RA, Subramani S: **A novel, cleavable peroxisomal targeting signal at the amino-terminus of the rat 3-ketoacyl-CoA thiolase.***EMBO J* 1991, **10**:3255–3262.

15. Edward Purdue P, Yang X, Lazarow PB: **Pex18p and Pex21p, a novel pair of related peroxins essential for peroxisomal targeting by the PTS2 pathway**. *J Cell Biol* 1998, **143**:1859–1869.

16. Otzen M, Wang D, Lunenborg MGJ, Klei IJ van der: ***Hansenula polymorpha* Pex20p is an oligomer that binds the peroxisomal targeting signal 2 (PTS2)**. *J Cell Sci* 2005, **118**:3409–3418.

17. Brown L-A, Baker A: **Shuttles and cycles: transport of proteins into the peroxisome matrix (Review)**. *Mol Membr Biol* 2008, **25**:363–375.

18. Erdmann R, Schliebs W: **Peroxisomal matrix protein import: the transient pore model**. *Nat Rev Mol Cell Biol* 2005, **6**:738–742.

19. Meinecke M, Cizmowski C, Schliebs W, Krüger V, Beck S, Wagner R, Erdmann R: **The peroxisomal importomer constitutes a large and highly dynamic pore**. *Nat Cell Biol* 2010, **12**:273–277.

20. Platta HW, Girzalsky W, Erdmann R: **Ubiquitination of the peroxisomal import receptor Pex5p**. *Biochem J* 2004, **384**:37–45.

21. Platta HW, Magraoui FE, Schlee D, Grunau S, Girzalsky W, Erdmann R: **Ubiquitination of the peroxisomal import receptor Pex5p is required for its recycling**. *J Cell Biol* 2007, **177**:197–204.

22. Platta HW, Grunau S, Rosenkranz K, Girzalsky W, Erdmann R: **Functional role of the AAA peroxins in dislocation of the cycling PTS1 receptor back to the cytosol**. *Nat Cell Biol* 2005, **7**:817–822.

23. Schmidt F, Treiber N, Zocher G, Bjelic S, Steinmetz MO, Kalbacher H, Stehle T, Dodt G: **Insights into Peroxisome Function from the Structure of Pex3 in Complex with a Soluble Fragment of Pex19**. *J Biol Chem* 2010, **285**:25410–25417.

24. Schueller N, Holton SJ, Fodor K, Milewski M, Konarev P, Stanley WA, Wolf J, Erdmann R, Schliebs W, Song Y-H, Wilmanns M: **The peroxisomal receptor Pex19p forms a helical mPTS recognition domain**. *EMBO J* 2010, **29**:2491–2500.

25. Thoms S, Harms I, Kalies K-U, Gärtner J: **Peroxisome formation requires the endoplasmic reticulum channel protein Sec61**. *Traffic* 2012, **13**:599–609.

26. Zand A van der, Braakman I, Tabak HF: **Peroxisomal membrane proteins insert into the endoplasmic reticulum**. *Mol Biol Cell* 2010, **21**:2057–2065.

27. Schuldiner M, Metz J, Schmid V, Denic V, Rakwalska M, Schmitt HD, Schwappach B, Weissman JS: **The GET Complex mediates insertion of tail-anchored proteins into the ER membrane**. *Cell* 2008, **134**:634–645.

28. Grabenbauer M, Sätzler K, Baumgart E, Fahimi HD: **Three-dimensional ultrastructural analysis of peroxisomes in HepG2 cells**. *Cell Biochem Biophys* 2000, **32**:37–49.

29. Schrader M, Fahimi HD: **Peroxisomes and oxidative stress**. *Biochim Biophys Acta BBA - Mol Cell Res* 2006, **1763**:1755–1766. [*Peroxisomes: Morphology, Function, Biogenesis and Disorders*]

30. Opalinski L, Kiel JAKW, Williams C, Veenhuis M, van der Klei IJ: **Membrane curvature during peroxisome fission requires Pex11**. *EMBO J* 2011, **30**:5–16.

31. Koch A, Yoon Y, Bonekamp NA, McNiven MA, Schrader M: **A role for Fis1 in both mitochondrial and peroxisomal fission in mammalian Cells**. *Mol Biol Cell* 2005, **16**:5077–5086.

32. Motley AM, Ward GP, Hettema EH: **Dnm1p-dependent peroxisome fission requires Caf4p, Mdv1p and Fis1p**. *J Cell Sci* 2008, **121**:1633–1640.

33. Koch A, Thiemann M, Grabenbauer M, Yoon Y, McNiven MA, Schrader M: **Dynamin-like protein 1 is involved in peroxisomal fission**. *J Biol Chem* 2003, **278**:8597–8605.

34. Hoepfner D, Berg M van den, Philippsen P, Tabak HF, Hettema EH: **A role for Vps1p, actin, and the Myo2p motor in peroxisome abundance and inheritance in *Saccharomyces cerevisiae***. *J Cell Biol* 2001, **155**:979–990.

35. Tuller G, Nemec T, Hrastnik C, Daum G: **Lipid composition of subcellular membranes of an FY1679-derived haploid yeast wild-type strain grown on different carbon sources**. *Yeast* 1999, **15**:1555–1564.

36. Zinser E, Sperka-Gottlieb CD, Fasch EV, Kohlwein SD, Paltauf F, Daum G: **Phospholipid synthesis and lipid composition of subcellular membranes in the unicellular eukaryote *Saccharomyces cerevisiae*.***J Bacteriol* 1991, **173**:2026–2034.

37. Horvath SE, Daum G: **Lipids of mitochondria**. *Prog Lipid Res* 2013, **52**:590–614.

38. Hardeman D, Versantvoort C, van den Brink JM, van den Bosch H: **Studies on peroxisomal membranes**. *Biochim Biophys Acta BBA - Biomembr* 1990, **1027**:149–154.

39. Quiñones W, Urbina JA, Dubourdieu M, Luis Concepción J: **The glycosome membrane of *Trypanosoma cruzi* epimastigotes: protein and lipid composition**. *Exp Parasitol* 2004, **106**:135–149.

40. Wriessnegger T, Gübitz G, Leitner E, Ingolic E, Cregg J, de la Cruz BJ, Daum G: **Lipid composition of peroxisomes from the yeast *Pichia pastoris* grown on different carbon sources**. *Biochim Biophys Acta BBA - Mol Cell Biol Lipids* 2007, **1771**:455–461.

41. Rosenberger S, Connerth M, Zellnig G, Daum G: **Phosphatidylethanolamine synthesized by three different pathways is supplied to peroxisomes of the yeast *Saccharomyces cerevisiae***. *Biochim Biophys Acta BBA - Mol Cell Biol Lipids* 2009, **1791**:379–387.

42. Nuttley WM, Bodnar AG, Mangroo D, Rachubinski RA: **Isolation and characterization of membranes from oleic acid-induced peroxisomes of *Candida tropicalis***. *J Cell Sci* 1990, **95**:463–470.

43. Fujiki Y, Fowler S, Shio H, Hubbard AL, Lazarow PB: **Polypeptide and phospholipid composition of the membrane of rat liver peroxisomes: comparison with endoplasmic reticulum and mitochondrial membranes.***J Cell Biol* 1982, **93**:103–110.

44. Pan R, Jones AD, Hu J: **Cardiolipin-mediated mitochondrial dynamics and stress response in *Arabidopsis***. *Plant Cell Online* 2014:tpc.113.121095.

45. Baile MG, Lu Y-W, Claypool SM: **The topology and regulation of cardiolipin biosynthesis and remodeling in yeast**. *Chem Phys Lipids* 2014, **179**:25–31. [*Progress in Cardiolipinomics*]

46. Mejia EM, Nguyen H, Hatch GM: **Mammalian cardiolipin biosynthesis**. *Chem Phys Lipids* 2014, **179**:11–16. [*Progress in Cardiolipinomics*]

47. Cullis PR, Verkleij AJ, Ververgaert PHJT: **Polymorphic phase behaviour of cardiolipin as detected by 31P NMR and freeze-fracture techniques. Effects of calcium, dibucaine and chlorpromazine**. *Biochim Biophys Acta BBA - Biomembr* 1978, **513**:11–20.

48. DeVay RM, Dominguez-Ramirez L, Lackner LL, Hoppins S, Stahlberg H, Nunnari J: **Coassembly of Mgm1 isoforms requires cardiolipin and mediates mitochondrial inner membrane fusion**. *J Cell Biol* 2009, **186**:793–803.

49. Joshi AS, Thompson MN, Fei N, Hutteman M, Greenberg ML: **Cardiolipin and mitochondrial phosphatidylethanolamine have overlapping functions in mitochondrial fusion in *Saccharomyces cerevisiae***. *J Biol Chem* 2012:jbc.M111.330167.

50. Mileykovskaya E, Dowhan W: **Cardiolipin membrane domains in prokaryotes and eukaryotes**. *Biochim Biophys Acta BBA - Biomembr* 2009, **1788**:2084–2091. [*Includes Special Section: Cardiolipin*]

51. Kutik S, Rissler M, Guan XL, Guiard B, Shui G, Gebert N, Heacock PN, Rehling P, Dowhan W, Wenk MR, Pfanner N, Wiedemann N: **The translocator maintenance protein Tam41 is required for mitochondrial cardiolipin biosynthesis**. *J Cell Biol* 2008, **183**:1213–1221.

52. Gonzalvez F, Gottlieb E: **Cardiolipin: Setting the beat of**. *Apoptosis* 2007, **12**:877–885.

53. Zhang M, Mileykovskaya E, Dowhan W: **Gluing the Respiratory Chain Together cardiolipin is required for supercomplex formation in the inner mitochondrial membrane**. *J Biol Chem* 2002, **277**:43553–43556.

54. Pfeiffer K, Gohil V, Stuart RA, Hunte C, Brandt U, Greenberg ML, Schägger H: **Cardiolipin stabilizes respiratory chain supercomplexes**. *J Biol Chem* 2003, **278**:52873–52880.

55. Zhong Q, Gohil VM, Ma L, Greenberg ML: **Absence of cardiolipin results in temperature sensitivity, respiratory defects, and mitochondrial DNA instability independent of Pet56**. *J Biol Chem* 2004, **279**:32294–32300.

56. Zhong Q, Gvozdenovic-Jeremic J, Webster P, Zhou J, Greenberg ML: **Loss of function of KRE5 suppresses temperature sensitivity of mutants lacking mitochondrial anionic lipids**. *Mol Biol Cell* 2005, **16**:665–675.

57. Zhong Q, Li G, Gvozdenovic-Jeremic J, Greenberg ML: **Up-regulation of the cell integrity pathway in *Saccharomyces cerevisiae* suppresses temperature sensitivity of the pgs1Δ Mutant**. *J Biol Chem* 2007, **282**:15946–15953.

58. Chen S, Tarsio M, Kane PM, Greenberg ML: **Cardiolipin mediates cross-talk between mitochondria and the vacuole**. *Mol Biol Cell* 2008, **19**:5047–5058.

59. Zhou J, Zhong Q, Li G, Greenberg ML: **Loss of cardiolipin leads to longevity defects that are alleviated by alterations in stress response signaling**. *J Biol Chem* 2009, **284**:18106–18114.

60. Cullis PR, De Kruijff B: **Lipid polymorphism and the functional roles of lipids in biological membranes**. *Biochim Biophys Acta BBA - Rev Biomembr* 1979, **559**:399–420.

61. Lindblom G, Rilfors L: **Nonlamellar phases formed by membrane lipids**. *Adv Colloid Interface Sci* 1992, **41**:101–125.

62. Birner R, Bürgermeister M, Schneiter R, Daum G: **Roles of phosphatidylethanolamine and of its several biosynthetic pathways in *Saccharomyces cerevisiae***. *Mol Biol Cell* 2001, **12**:997–1007.

63. Birner R, Nebauer R, Schneiter R, Daum G: **Synthetic lethal interaction of the mitochondrial phosphatidylethanolamine biosynthetic machinery with the prohibitin Complex of *Saccharomyces cerevisiae***. *Mol Biol Cell* 2003, **14**:370–383.

64. Ichimura Y, Kirisako T, Takao T, Satomi Y, Shimonishi Y, Ishihara N, Mizushima N, Tanida I, Kominami E, Ohsumi M, Noda T, Ohsumi Y: **A ubiquitin-like system mediates protein lipidation**. *Nature* 2000, **408**:488–492.

65. Rilfors L, Lindblom G, Wieslander Å, Christiansson A: **Lipid bilayer stability in biological membranes**. In *Membr Fluidity*. Edited by Kates M, Manson LA. Springer US; 1984:205–245. [*Biomembranes*, vol. 12]

66. Zheng Z, Zou J: **The initial step of the glycerolipid pathway identification of glycerol 3-phosphate/dihydroxyacetone phosphate dual substrate acyltransferases in *Saccharomyces cerevisiae***. *J Biol Chem* 2001, **276**:41710–41716.

67. Athenstaedt K, Daum G: **1-Acyldihydroxyacetone-phosphate reductase (Ayr1p) of the yeast *Saccharomyces cerevisiae* encoded by the open reading frame YIL124w is a major component of lipid particles**. *J Biol Chem* 2000, **275**:235–240.

68. Benghezal M, Roubaty C, Veepuri V, Knudsen J, Conzelmann A: **SLC1 and SLC4 encode partially redundant acyl-Coenzyme A 1-acylglycerol-3-phosphate o-acyltransferases of budding yeast**. *J Biol Chem* 2007, **282**:30845–30855.

69. Shen H, Heacock PN, Clancey CJ, Dowhan W: **The *CDS1*gene encoding CDP-diacylglycerol synthase in *Saccharomyces cerevisiae*is essential for cell growth**. *J Biol Chem* 1996, **271**:789–795.

70. Kuchler K, Daum G, Paltauf F: **Subcellular and submitochondrial localization of phospholipid-synthesizing enzyme in *Saccharomyces cerevisiae***. *J Bacteriol* 1986, **165**:901–910.

71. Chang S-C, Heacock PN, Clancey CJ, Dowhan W: **The *PEL1* Gene (Renamed *PGS1*) Encodes the phosphatidylglycero-phosphate synthase of*Saccharomyces cerevisiae***. *J Biol Chem* 1998, **273**:9829–9836.

72. Osman C, Haag M, Wieland FT, Brügger B, Langer T: **A mitochondrial phosphatase required for cardiolipin biosynthesis: the PGP phosphatase Gep4**. *EMBO J* 2010, **29**:1976–1987.

73. Jiang F, Rizavi HS, Greenberg ML: **Cardiolipin is not essential for the growth of *Saccharomyces cerevisiae* on fermentable or non-fermentable carbon sources**. *Mol Microbiol* 1997, **26**:481–491.

74. Letts VA, Klig LS, Bae-Lee M, Carman GM, Henry SA: **Isolation of the yeast structural gene for the membrane-associated enzyme phosphatidylserine synthase**. *Proc Natl Acad Sci* 1983, **80**:7279–7283.

75. Trotter PJ, Voelker DR: **Identification of a non-mitochondrial phosphatidylserine decarboxylase activity (PSD2) in the yeast *Saccharomyces cerevisiae***. *J Biol Chem* 1995, **270**:6062–6070.

76. Trotter PJ, Pedretti J, Voelker DR: **Phosphatidylserine decarboxylase from *Saccharomyces cerevisiae*. Isolation of mutants, cloning of the gene, and creation of a null allele**. *J Biol Chem* 1993, **268**:21416–21424.

77. Kim K, Kim K-H, Storey MK, Voelker DR, Carman GM: **Isolation and characterization of the *Saccharomyces cerevisiaeEKI1* Gene Encoding ethanolamine kinase**. *J Biol Chem* 1999, **274**:14857–14866.

78. Min-Seok R, Kawamata Y, Nakamura H, Ohta A, Takagi M: **Isolation and characterization of *ECT1* gene encoding CTP: phosphoethanolamine cytidylyltransferase of *Saccharomyces cerevisiae***. *J Biochem (Tokyo)* 1996, **120**:1040–1047.

79. Hjelmstad RH, Bell RM: **The sn-1,2-diacylglycerol ethanolaminephosphotransferase activity of *Saccharomyces cerevisiae*. Isolation of mutants and cloning of the EPT1 gene.***J Biol Chem* 1988, **263**:19748–19757.

80. Hjelmstad RH, Bell RM: **sn-1,2-diacylglycerol choline- and ethanolaminephosphotransferases in *Saccharomyces cerevisiae*: Nucleotide sequence of the *EPT1* gene and comparison of the *CPT1* and *EPT1* gene products**. *J Biol Chem* 1991, **266**:5094–5103.

81. Saba JD, Nara F, Bielawska A, Garrett S, Hannun YA: **The *BST1* Gene of *Saccharomyces cerevisiae*is the sphingosine-1-phosphate lyase**. *J Biol Chem* 1997, **272**:26087–26090.

82. Gottlieb D, Heideman W, Saba JD: **The*DPL1*Gene is involved in mediating the response to nutrient deprivation in*Saccharomyces cerevisiae***. *Mol Cell Biol Res Commun* 1999, **1**:66–71.

83. Raychaudhuri S, Prinz WA: **Nonvesicular phospholipid transfer between peroxisomes and the endoplasmic reticulum**. *Proc Natl Acad Sci U S A* 2008, **105**:15785–15790.

84. Wirtz KWA: **Phospholipid transfer proteins**. *Annu Rev Biochem* 1991, **60**:73–99.

85. Neuspiel M, Schauss AC, Braschi E, Zunino R, Rippstein P, Rachubinski RA, Andrade-Navarro MA, McBride HM: **Cargo-selected transport from the mitochondria to peroxisomes is mediated by vesicular carriers**. *Curr Biol* 2008, **18**:102–108.

86. Elbaz Y, Schuldiner M: **Staying in touch: the molecular era of organelle contact sites**. *Trends Biochem Sci* 2011, **36**:616–623.

87. Rowland AA, Voeltz GK: **Endoplasmic reticulum–mitochondria contacts: function of the junction**. *Nat Rev Mol Cell Biol* 2012, **13**:607–625.

88. Tatsuta T, Scharwey M, Langer T: **Mitochondrial lipid trafficking**. *Trends Cell Biol* 2014, **24**:44–52. [*Special Issue: Membrane Trafficking*]

89. Klecker T, Böckler S, Westermann B: **Making connections: interorganelle contacts orchestrate mitochondrial behavior**. *Trends Cell Biol* .

90. Achleitner G, Gaigg B, Krasser A, Kainersdorfer E, Kohlwein SD, Perktold A, Zellnig G, Daum G: **Association between the endoplasmic reticulum and mitochondria of yeast facilitates interorganelle transport of phospholipids through membrane contact**. *Eur J Biochem FEBS* 1999, **264**:545–553.

91. Van Dijken JP, Otto R, Harder W: **Growth of *Hansenula polymorpha* in a methanol-limited chemostat. Physiological responses due to the involvement of methanol oxidase as a key enzyme in methanol metabolism**. *Arch Microbiol* 1976, **111**:137–144.

92. Faber KN, Haima P, Harder W, Veenhuis M, AB G: **Highly-efficient electrotransformation of the yeast *Hansenula polymorpha***. *Curr Genet* 1994, **25**:305–310.

93. Gietz D, St Jean A, Woods RA, Schiestl RH: **Improved method for high efficiency transformation of intact yeast cells**. *Nucleic Acids Res* 1992, **20**:1425.

94. Saraya R, Krikken AM, Kiel JAKW, Baerends RJS, Veenhuis M, van der Klei IJ: **Novel genetic tools for *Hansenula polymorpha***. *FEMS Yeast Res* 2012, **12**:271–278.

95. Wriessnegger T, Gübitz G, Leitner E, Ingolic E, Cregg J, de la Cruz BJ, Daum G: **Lipid composition of peroxisomes from the yeast *Pichia pastoris* grown on different carbon sources**. *Biochim Biophys Acta BBA - Mol Cell Biol Lipids* 2007, **1771**:455–461.

96. Cohen Y, Klug YA, Dimitrov L, Erez Z, Chuartzman SG, Elinger D, Yofe I, Soliman K, Gärtner J, Thoms S, Schekman R, Elbaz-Alon Y, Zalckvar E, Schuldiner M: **Peroxisomes are juxtaposed to strategic sites on mitochondria**. *Mol Biosyst* 2014, **10**:1742–1748.

97. Saraya R, Krikken AM, Veenhuis M, Klei IJ van der: **Peroxisome reintroduction in *Hansenula polymorpha* requires Pex25 and Rho1**. *J Cell Biol* 2011, **193**:885–900.

98. Nagotu S, Saraya R, Otzen M, Veenhuis M, van der Klei IJ: **Peroxisome proliferation in *Hansenula polymorpha* requires Dnm1p which mediates fission but not de novo formation**. *Biochim Biophys Acta BBA - Mol Cell Res* 2008, **1783**:760–769.

99. Guldener U, Heck S, Fielder T, Beinhauer J, Hegemann JH: **A new efficient gene disruption cassette for repeated use in budding yeast.***Nucleic Acids Res* 1996, **24**:2519–2524.

100. Baerends RJS, Faber KN, Kram AM, Kiel JAKW, Klei IJ van der, Veenhuis M: **A stretch of positively charged amino acids at the N terminus of*Hansenula polymorpha* Pex3p is involved in incorporation of the protein into the peroxisomal membrane**. *J Biol Chem* 2000, **275**:9986–9995.

101. Cepińska MN, Veenhuis M, van der Klei IJ, Nagotu S: **Peroxisome fission is associated with reorganization of specific membrane proteins**. *Traffic* 2011, **12**:925–937.